

Simulation of a Badminton Racket

A parametric study of racket design parameters using Finite Element Analysis.

Master's thesis in Applied Mechanics

ELIAS BLOMSTRAND

MIKE DEMANT

MASTER'S THESIS IN APPLIED MECHANICS

Simulation of a Badminton Racket

A parametric study of racket design parameters using Finite Element Analysis.

ELIAS BLOMSTRAND
MIKE DEMANT

Department of Applied Mechanics
Division of Solid Mechanics
CHALMERS UNIVERSITY OF TECHNOLOGY
Göteborg, Sweden 2017

Simulation of a Badminton Racket

A parametric study of racket design parameters using Finite Element Analysis.

ELIAS BLOMSTRAND

MIKE DEMANT

© ELIAS BLOMSTRAND, MIKE DEMANT, 2017

Master's thesis 2017:52

ISSN 1652-8557

Department of Applied Mechanics

Division of Solid Mechanics

Chalmers University of Technology

SE-412 96 Göteborg

Sweden

Telephone: +46 (0)31-772 1000

Cover:

Illustration of a smash sequence for a badminton racket.

Chalmers Reproservice

Göteborg, Sweden 2017

Simulation of a Badminton Racket

A parametric study of racket design parameters using Finite Element Analysis.

Master's thesis in Applied Mechanics

ELIAS BLOMSTRAND

MIKE DEMANT

Department of Applied Mechanics

Division of Solid Mechanics

Chalmers University of Technology

ABSTRACT

Badminton, said to be the worlds fastest ball sport, is a fairly unknown sport from a scientific point of view. There has been great progress made to get from the old wooden rackets of the 19th century to the light-weight high performance composite ones used today, but the development process is based on a trial and error method rather than on scientific knowledge. The limited amount of existing studies indicate that racket parameters like shaft stiffness, center of gravity and head geometry affect the performance of the racket greatly. These studies have either been physical test with limit number of data points or simplified computer simulations.

In this work a parametric study of racket models is performed with the purpose to find key racket design parameters using Finite Element Analysis, FEA. Eleven racket models are simulated using one smash and one clear swing. One is the reference model, based on a modern isometric racket, and the other ten have one parameter modified to see how this alters the response. In addition to the swing tests, the sweet spots of the racket head is analysed and the eigenmodes of the racket are investigated.

The results show that the previously mentioned parameters have a noticeable effect on racket performance. A low shaft stiffness may give higher shuttle velocities if used correctly, and an inconsistent shuttle speed and trajectory if used incorrectly. High center of gravity has a less inconsistent effect but instead would require more effort to swing. Noticeable is that the Y-shaped head introduced by Prince, which since has been removed from the market, perform very well in some aspects. These results show that FEA should be seen as a useful tool in badminton racket development and with further work on the field advances can be made that would make badminton the definitive fastest ball sport in the world.

Keywords: Badminton, Racket, Composite, FEA, FEM, LS-Dyna, Smash, Clear, Sweet spot

PREFACE

This thesis treat the possibility to adapt an CAE method for design and evaluate badminton racket. The study is performed at the engineering consultant firm FS Dynamics with the sports equipment company Salming as the end costumer. The project was carried out during the spring semester 2017 corresponding 20 week for each of the two participants. The final examination was done at the department of Applied Mechanics at Chalmers University of Technology with Martin Fagerström as the accountable examiner.

ACKNOWLEDGEMENTS

First and foremost our gratitude goes towards FS Dynamics who gave us the opportunity to work with this project together with the end costumer Salming. Many thanks to our supervisors at FS-Dynamics, Björn Andersson and Mattias Wångblad, for providing us with valuable feedback and guidance throughout the project. Further we like to thank Linus Lindgren for helping us with several issues in the software LS-Dyna. An additionally gratitude towards Maxine Kwan and John Rasmussen for providing us with the motion capture data. Finally a special thank to our examiner at Chalmers University of Technology, Martin Fagerström.

CONTENTS

Abstract	i
Preface	iii
Acknowledgements	iii
Contents	v
1 Introduction	1
1.1 Purpose	1
1.2 Objective	1
1.3 Limitations	2
1.4 The Game of Badminton	2
1.4.1 Badminton Racket	3
1.4.2 Shuttlecock	3
1.4.3 Badminton Strokes	4
1.4.4 The Player	4
2 Theory	5
2.1 Racket Properties	5
2.1.1 Racket Mass and Swing-Weight	5
2.1.2 Racket Stiffness	6
2.1.3 String Properties	7
2.2 Key Parameters for Racket Design	7
2.3 Challenges Due to Individual Player Characteristics	8
2.4 Finite Element Method	8
2.4.1 Mesh	8
2.4.2 Hourglass	9
2.4.3 Elements	10
2.5 Composite Mechanics	10
2.5.1 FE-model of Composite Materials	11
2.6 Motion Capture	12
3 Method	13
3.1 Used Software Products	13
3.2 Racket Motion	14
3.3 CAD Model for the Racket	14
3.3.1 CAD Model for the Head and the Shaft	15
3.3.2 CAD Model for the Net	15
3.3.3 CAD Model for the Handle	15
3.3.4 CAD Model for the Shuttle	16
3.4 Material Properties	16
3.4.1 Static Bending Test for Material Verification	16
3.4.2 Composite Material for Frame	17
3.4.3 Wood Material for Handle	17
3.4.4 Material for Strings	17
3.4.5 Cork Material for Shuttle	17
3.5 The Finite Element Model of the Racket	18
3.5.1 Defining Part Identities (PID)	18
3.5.2 Meshing Procedure and Used Element Formulations	18
3.5.3 FE-model of the Badminton Racket	19
3.5.4 Alternations for Model Used in the Implicit Eigenmode Analysis	22
3.5.5 Alternations for Rigid FE-model	22
3.6 Parameter Study	22
3.7 Simulations	23
3.7.1 Simulation Settings	23
3.7.2 Execute Simulation	24
3.7.3 Eigenfrequency Analysis	24
3.7.4 Deflection Analysis	25

3.7.5	Sweet Spot Analysis for Swing	25
3.7.6	Sweet Spot for Clamped Racket	25
3.7.7	Time Window Analysis for Shuttle Impact	26
3.8	Method for Post-process and Organise Data	26
3.8.1	Post-processing Result in Meta	26
3.9	Post-processing in MATLAB	27
3.9.1	Comparison of Input and Output	27
3.9.2	Deflection of the Racket	27
3.9.3	Shuttle Motion and Contact	28
3.9.4	Sweet Spot Analysis	28
4	Result	29
4.1	Racket Motion	29
4.2	Static Deflection Test	30
4.3	Mesh Convergence	31
4.4	Frequency Response and Eigenfrequencies	31
4.5	Clear - Racket Behaviour and Parameter Influence	32
4.5.1	Deflection of Racket During Swing and Hit	32
4.5.2	Racket Velocity at Impact	33
4.5.3	Momentum During Stroke	35
4.5.4	Contact Time and Duration	35
4.5.5	Shuttle Velocity and Direction	37
4.5.6	Repositioned Ball	37
4.6	Smash - Racket Behaviour and Parameter Influence	38
4.6.1	Deflection	38
4.6.2	Racket Velocity at Impact	39
4.6.3	Momentum During Stroke	41
4.6.4	Contact Time and Duration	42
4.6.5	Shuttle Velocity and Direction	42
4.6.6	Repositioned Ball	43
4.7	Sweet Spot Analysis for Clamped Racket	44
5	Discussion	46
5.1	Racket Motion	46
5.2	Calibration of FE-model	46
5.3	The Natural Frequency Response	47
5.4	Racket Responses for Key Parameter Variations	47
5.4.1	Centre of Gravity	47
5.4.2	Mass	48
5.4.3	Shaft Stiffness	48
5.4.4	Head Stiffness	49
5.4.5	Geometry	49
5.5	FE-model and Material Properties	50
5.6	Assumptions and Other Sources of Error	50
6	Conclusion	52
7	Future Work	54
	References	55
A	Tables	I
B	Sweet Spots	V

1

Introduction

Badminton is said to be the worlds fastest ball game [1] where the increase in the pace of the game has mainly been dependent on new available materials [2]. However, the effect from different parameters such as stiffness, weight distribution, tension in the strings etc. on the speed of the game is yet poorly understood [3]. Manufacturers work by improving on the latest model of rackets based on player feedback and experience, rather than using scientific methods [4]. This trial and error type of development does not guarantee the best design and is probable to occasionally fail. With greater scientific understanding of which parameters that affect the performance of the badminton racket, and in which way, the development process could be made more accurate. By identification of the impact of each parameter, rackets could also be further personalised. This is of interest for manufacturers of high-performance rackets to provide players with an optimised racket.

Salming Sports is a manufacturer of premium sports equipment and acknowledged actor in the squash business with clothes, shoes and rackets. With similar demands on equipment in the sport of badminton the company has begun to expand into this market as well. But before they start manufacturing badminton rackets they want deeper insight into what makes a racket high performing. Salming base their products on quantitative facts, whereby it is important to have an understanding of the racket dynamics and the performance due to different parameters.

FS Dynamics is a Computer Aided Engineering (CAE) supplier based in Scandinavia which has been tasked by Salming to provide the CAE analysis of the racket mechanics. This project is a collaboration between FS Dynamics and Salming and is conducted as a master thesis at the Department of Applied Mechanics at Chalmers University of Technology.

1.1 Purpose

The purpose of this thesis is to identify key parameters pertaining to racket dynamics using Finite Element Analysis (FEA) and to develop a greater understanding of their influence. The FEA will be performed using LS-Dyna as an explicit FEA solver. The result can be used as a scientific basis in the racket design process, and will be used to show if FEA is a valid tool in badminton racket design and optimisation. The end goal of this thesis is not to develop a racket, but to identify and define a comprehensive summary of the governing racket dynamic parameters.

1.2 Objective

The objective of this project is to identify key properties of the racket design and how they change the characteristics of the racket. The resulting insight will give more information to the racket design process and further demonstrate the usability of CAE within badminton racket development. To complete this, the following milestones have been set:

- Identify key properties that govern the badminton racket characteristics.
- Have data for a smash and a clear swing to add the motion into the FE-analysis.
- Define suitable geometry and material data to include in the model.

- Define and validate the FE-model of a badminton racket.
- Simulate the defined motions using the explicit solver in LS-Dyna.
- Perform a parametric study of the variations on the racket model and evaluate the impact of the racket design parameters.

1.3 Limitations

The work in this project is carried out by two persons and is limited to 20 weeks. These limitations have been set for the objectives to be achievable:

- String properties are not evaluated, i.e. the same properties and pre-loading for the strings are used for all models.
- Geometrical variations is limited to variations of the so called isometric racket shape, see Figure 1.2.
- All variations of racket parameters are kept within ranges allowed by the rules set by Badminton World Federation [5].
- The simulation is limited to the two strokes smash and clear.
- Each stroke is limited to one movement pattern each, i.e. different players and individual variation is not considered.
- No material data is available, thus the material properties is chosen using calibration methods.
- The FEA does not contain any air resistance.

1.4 The Game of Badminton

The game of badminton has been played since the middle of the 19th century and in 1992 it became part of the Olympic Summer Games [6]. The objective of the game, as stated in the Badminton Laws [5], is to score points by landing the ball, named shuttlecock and shown in Figure 1.3, on the opposition's part of the court. The shuttle may only be hit using a badminton racket, see Figure 1.2 for an illustration of a badminton racket. Dividing the court is a net which the shuttle has to pass over before hitting the ground of the adversary, see Figure 1.1. Any attempt to hit the shuttle where it does not pass over the net or does land outside of the opponent's court is a foul which grants the opponent the point. As the shuttle passes over the net the opponent must prevent the ball from touching the ground on their side by shooting it back over the net and, hopefully, hitting the ground of the first player's court to score a point. Each side is only allowed one touch of the shuttle before it must pass over the net. The game can be played as single or double with one or two players per side respectively.

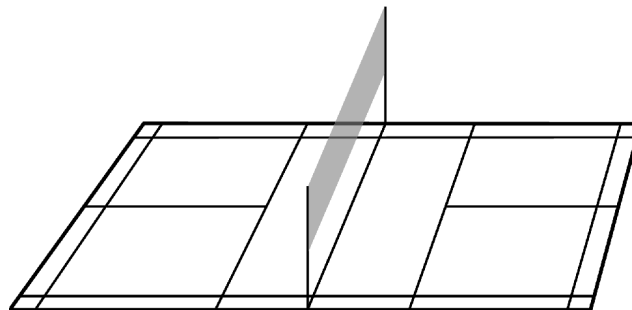


Figure 1.1: A badminton court.



Figure 1.2: *Modern badminton racket, isometric shape. It consists of the handle, shaft, head and string bed.*



Figure 1.3: *Shuttlecocks. To the left a plastic shuttle and to the right a feathered shuttle.*

1.4.1 Badminton Racket

The badminton racket originally was constructed by fitting a net made out of parchment or catgut to a wooden frame [7]. Since then the sport has developed to a fast paced game, much due to the improvements in racket design. The modern racket is made primarily out of a composite material [2] which allows for a stiff, lightweight construction. The strings are usually made of a polymer which can hold a strong tension, normally between 90-140 N [8]. There are two head shapes in use: an oval shape and an isometric shape, seen in Figure 1.2 where the traditional oval shape has been stretched to become more square. Isometric is the used abbreviation of the full name "Isometric square head shape" which the manufacturer Yonex named it, and claimed it gave a bigger sweet spot than the oval shape. While many parts of the racket have been modernised with the development of the sport the handle is still made out of wood.

Racket Regulations

The design of the racket is limited by regulations defined by the Badminton World Federation [5]. These specify that:

1. the overall length may not be longer than 680 mm.
2. the overall width may not be wider than 230 mm.
3. the overall length of the stringed area may not be longer than 280 mm.
4. the overall width of the stringed area may not be wider than 220 mm.
5. the stringing pattern shall be generally uniform, particularly not less dense in the center than elsewhere.
6. the stringed area may extend into an area connecting the head with the shaft, provided that:
 - (a) the width of the extended area does not exceed 35 mm.
 - (b) the overall length of the stringed area does not then exceed 330 mm.

The stringed area is defined as the area within the head i.e. the string bed. There are more rules regarding the racket, but these do not apply to this study.

1.4.2 Shuttlecock

The ball used in badminton is called a shuttle, short for shuttlecock, which has two significant parts: the feather cone and the sturdy cork base. The cone feather structure is either made from real feathers or a more durable plastic skirt, as shown in Figure 1.3. While the real feather type is more expensive than the synthetic it also has less variations in flight characteristics [9], which is why it is normally used in competitive games. The structure of the shuttle makes it aerodynamically stable with high drag properties, a necessity for an opponent to be able to hit the flying projectile which has been recorded to have a maximum speed of 113 m/s [10].

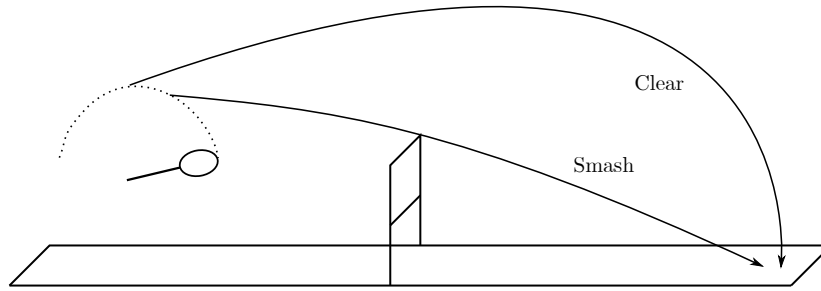


Figure 1.4: *The clear and smash badminton stroke.*

1.4.3 Badminton Strokes

In a game of badminton, several distinct badminton strokes are used which each has its specific purpose. Two of the most common strokes are the clear and the smash stroke, see Figure 1.4. The first is a generally used as a defensive move where the shuttle is given a high upwards velocity, arcing over the court, and is only reachable by the opposing player as it comes down again at the end of the court, furthest away from the net. From here it is usually easy for the opponent to hit the shuttle but hard for him to make an aggressive counter attack. This together with the fact that the player hitting the clear stroke will have time to re-position himself during the extra time it takes for the ball to return down to the court makes the clear a good defensive shot.

The second stroke, the smash, is an attacking move where the ball is hit with high velocity in a steep angle, giving the opponent less time to react and try to return the shuttle. There are more types of badminton strokes, but the aforementioned have been chosen to be used in this study due to the frequency of use and that they require a lot of power from the racket to be executed well.

1.4.4 The Player

A game of badminton contains a lot of variation where the player needs to make split second decisions on how to reach the shuttle before it touches their court and return it disadvantageously to the opponent, in the way the player personally sees as the optimal way. This action is greatly influenced by the player style, if he or she is a offensive or defensive player. An offensive player may try to position themselves more aggressively where he can return the shuttle before the opponent has re-positioned himself, using a more forceful swing than the defensive player would use. To quantify measurable properties and parameters of a badminton racket which influence the performance, it is vital to understand the game and be mindful of these existing different types of players.

Another property of the player which has a high impact on the game is the experience level of the player. The amount of experience defines whether a player is novice, recreational or an expert. The intention of this thesis is not to evaluate the difference between an inexperienced player and an expert, thus the focus will be to compare response and results with skilled players and their patterns. Although one observation by Kwan et. al. [4] is that recreational players tend to hit the shuttlecock in a later state having a positive deflection on the racket while an expert hits the shuttlecock with a negative deflection, see Figure 2.1. The distinction between an attacking or defending player also becomes more prominent with more experienced players.

In the studies by Lee et al. [11] and Tong et al. [12] the pattern regarding preferable strokes and the efficiency of these is measured for players from different matches in professional championships. The conclusion is that the most efficient and preferred stroke when trying to obtain a point, also referred as a kill shot, is the smash followed by the net shot. For the return strokes the net, drop and clear shot is the most efficient and thereby used shots. It is further discovered that male and female players prefers different techniques. The pattern among male players is dominated by smash and net shot whereas female players prefers drop and clear shots [11].

The characteristics of the strokes can be divided into power and control and by linking racket parameters to these actions an understanding how to design the racket to influence the most critical parts of badminton is achieved.

2

Theory

The technical development of badminton has increased the speed of the game since its inception. But rarely are these improvements based on scientific data, instead these are the result of trial and error. This study therefore uses data from studies on similar fields, e.g. tennis, in addition to the limited number of badminton studies. In this section, the current theories regarding racket properties are introduced. These, together with the necessary theory for the FE-model and motion capture, serve as the theoretical base for the method used in this project.

2.1 Racket Properties

Previous studies have mainly focused on the effect on racket performance based on weight, stiffnesses and string properties as variables. The following section provides a summary of the theories and results that define the foundation on which this study was based on.

2.1.1 Racket Mass and Swing-Weight

A modern racket weighs about 90 g with its centre of gravity (COG) located along the shaft axis, typically roughly half-way along the shaft. The position of the COG is shifted along the axis of the shaft by the manufacturers, which they claim changes the performance of the racket. It is said to be "head-heavy" if the COG is closer to the head and "head-light" if it is instead closer to the handle. The "head-heavy" model is marketed towards attacking players with the reason that it should give a more forceful swing, while its counterpart is angled towards the defending players as it should be easier to make fast reactive moves when the COG is closer to the hand of the player.

The reason why manoeuvring the racket is easier with a COG closer to the handle is that it lowers the racket's moment of inertia (MOI), given that the racket is held at the handle. The MOI determines how much torque is needed to give a rotational acceleration to the racket. It is calculated from the mass of each infinitely small point of the racket and the distance of the point from the rotational axis, which during the swing is at the handle. Thus, when the COG, also known as the centre of mass, is shifted towards the handle the MOI decreases and less torque is needed to swing the racket.

As mentioned in Section 1.4.1, the mass of the racket have decreased drastically by changing from the old wooden rackets to the modern composite rackets. As a consequence, the rackets can be swung faster with less effort. However as Hsieh et. al. observe in a study with two different rackets with the masses 100g and 85g, the heavier racket is faster to swing which indicates that weight reduction may only be beneficial until a certain point [13].

Based on this observation further evaluation is needed regarding how the head speed and the shuttle post impact speed correlates to the mass. Is the increased speed due to a heavier racket adequate to compensate for the extra energy needed to move the racket? The link between MOI, also referred to as swing-weight, and the velocity of the racket at impact needs to be further examined. Mitchell et. al. [14] imply that a correlation between MOI and the pre-impact racket speed exist but the result contradict each other between the participating players. Due to the low amount of players in their study and the diverging result, further evaluation to capture the correlation is needed. Nevertheless, the data is enough to indicate a possible theory. During a study by Cross et. al. [15] the result indicated that the swing speed of a racket with constant mass decreased as the moment of inertia increases, regardless if the player performs the swing using the forearm only or by also include the upper arm. However the magnitude of the influence was greater for a swing preformed

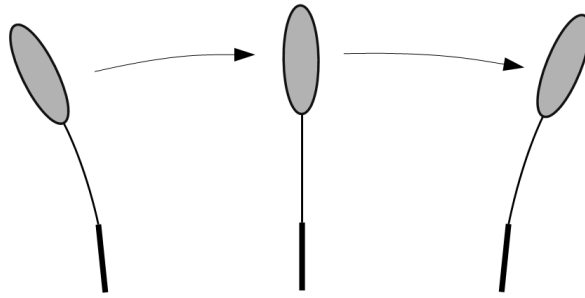


Figure 2.1: *Deflection of a racket during swing. Negative deflection at first when handle accelerates, at the end positive deflection.*

solely by the forearm. This is due to the fact that the total MOI for a forearm swing is dominated by the racket swing-weight.

To calculate the MOI for a badminton stroke the entire player-racket system needs to be considered to obtain the true value. This is a complex procedure since several individual aspects as play style, technique and pure bio-mechanical properties affect the result. For example, the rotation of elbow, shoulder and wrist can differ. Additionally, more or less wrist action is used by the player. Regarding the measurement of the swing-weight the usual approach is to measure the moment of inertia in a laboratory environment with the reference axis close to the end of the handle [15]. The true axis is dependent on the individual anatomic and play style, thus the result using the measured swing-weight might need to be calibrated to fit a specific player.

A conclusion from these studies is that changes in racket mass or baseball bat mass only have a small effect on the resulting shuttle speed. Although even small effects can have significant outcomes, improvement on a professional level is rarely measured in big numbers when it comes to accelerations or time etc. but can be the central difference from loosing to winning a point or even a match. As an example, Brody [16] showed that a tennis player is relatively sensitive to alternations of properties affecting the moment of inertia. Players in the study capture differences as low as 2.5% and further differences as small as 5% regarding the polar moment (the rackets ability to resist torsion).

2.1.2 Racket Stiffness

The elasticity of the racket is primarily inherited from the shaft's properties as it is where most of the bending of the racket occurs as the racket is swung [17]. To swing the racket a translating and/or rotating force is applied to the handle by the hand. Because the shaft is elastic, the distance between handle and head leads to a delay of the force affecting the head of the racket. Thus, the shaft will bend backwards initially during a swing, see Figure 2.1.

The timing window of the impact during a smash was identified in a study with both ranked and unranked players [17]. It was found that there was a 20 ms window in which the positive acceleration was at its maximum and the study participants hit the shuttle within 87 % of this time. The window was shown to shift position in relation to the start of the forward motion of the swing with different racket stiffness. Thus, a relatively small shift of stiffness can have an impact on optimal swing timing.

In Kwans research to design the worlds best badminton racket [4] the hypothesis is that the optimal racket stiffness could be identified as where stroke variation is minimal (maximising control) but with stiffness as flexible as possible (maximising power). It is also noted that the influence of elasticity can provide an additional 2-3 m/s to the racket head speed at impact. This contribution is more noticeable for novice players as their maximum head speed is generally lower than for advanced players, who in the studies achieve head speeds of 35 m/s. For advanced players, the greater variation in strokes due to higher compliance affects the control too much, leading to them preferring stiffer rackets due to the extra head speed gained from elasticity not outweighing the loss of control [17].

The rest of the racket, the head and handle, also have stiffness's which affect the performance of the racket. These have not been studied as extensively as the shaft stiffness but are likely to impact both the energy transfer to the shuttle and to the hand.

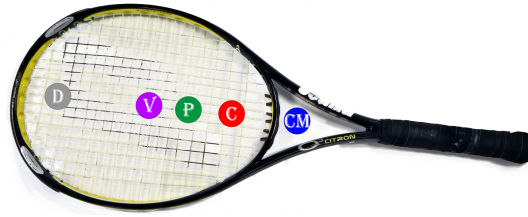


Figure 2.2: *Example of locations of specific tennis racket spots. CM = center mass, C = maximum COR, P = center of percussion, V = vibration node and D = dead spot. [20]*

2.1.3 String Properties

To show how the string bed affects the shuttle a measurement of the coefficient of restitution (COR) is often used. The relative speed of the shuttle and racket before and after impact are used to give the quotient COR as:

$$\text{COR} = \frac{v_2 - V_2}{V_1 - v_1}$$

where v are shuttle speeds and V racket speeds. Pre-impact speeds are indicated by the number 1, and post-impact by number 2. It was shown for a stationary racket that the COR value decreased with greater string tension in the range of 60-150 N in a FE-simulation study [3]. In this study, a ball was dropped on a racket with the rim of the head fixed. A physical study with a low number of participants indicated that string tension is not the only factor relevant for fast shuttle speeds [8]. The study found that more experienced players can somehow consistently achieve similar speeds with string tension in the range of 70-130 N.

Power is not the only property of the racket effected by the string tension. Control of the out-bounding ball from a tennis racket depends on the string tension [18]. It was shown that low string tension lead to problems controlling the speed of the shuttle post impact. The same researchers also noted in another study that 28% of the participants were sensitive to changes in string tension of the tennis racket [19].

The effects of impact between shuttle and racket, for example the shuttle velocity, is dependant on where on the string bed contact is made. The existence and locations of sweet spots on the bed is the main factor of this response [20]. Sweet spots are points or zones on the string bed where a characteristic of the impact is maximised when the shuttle collides into it, see Figure 2.2. The sweet spots can be defined as: the location of the maximum COR, the centre of percussion and the vibration node. The last two pertain to the vibrations and forces affecting the hand post-impact and are not studied in this thesis.

As the shuttle connects with the racket it is accelerated forward. This transfer of energy into the shuttle also induces a force on the racket which leads to vibrations in the racket handle. The noise produced during impact is an audial feedback of the racket [18]. This sound could indicate the efficiency of the racket and if the shuttle hit a sweet spot. The frequency of the feedback however is very dependent on string tension. It also results in a vibrations in the hand which can be used to sense the effectiveness of the hit.

2.2 Key Parameters for Racket Design

Previous studies indicate that specific racket design parameters are especially interesting to study for their impact on racket performance. These are:

- center of gravity, which is the main factor in determining the MOI of the racket. Studies show that this affects the swing properties more than other factors.
- weight, which should not affect the swing as much as COG. A greater weight should mean greater force applied to the shuttle resulting in higher outbound velocities.
- shaft stiffness, which determines how the shaft flexes during the swing. A less stiff shaft can lead to higher shuttle velocities but also a weak racket.
- head stiffness, which like the shaft stiffness impacts the tip deflection of the racket. Also may impact the shuttle velocity after impact.
- head shape, which affects the location of sweet spots on the string bead and the stiffness of the head.

The racket head shape is not the same for all racket sports. This could be because the sports differ in aspects like ball and court size, but could also be due to a history of development dominated by non-data based development. In Figure 2.3 three head shapes are shown where the isometric is the predominant one. The Y-shaped head was an attempt from the sports accessory company Prince which seems not to be available on the market anymore. The oval shape is less common than the isometric but is currently available on the market and is advertised to have be more powerful but at the cost of a smaller sweet spot.

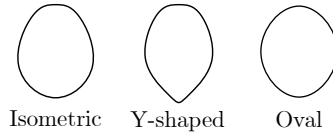


Figure 2.3: *Common racket sport head shapes.*

2.3 Challenges Due to Individual Player Characteristics

Badminton and other ball sports are high in variation due to the individual player aspects affecting the circumstances of the game. The shuttle is hit from different angles in different areas of the court at various speeds. On top of this, the player hitting the ball has his individual playing style; how he holds his racket, how fast he swings and how well he manages to hit the ball with the center of the rackets stringed area etc. As such, finding the optimal design of a racket could be described as pursuit to find the racket which performs best in all possible circumstances, which may be weighted by the likely-hood of that circumstance.

Another step of optimisation would be to design the racket to fit a certain player type, as suggested in Kwan's study to design the best racket [4]. This is done to an extent in the modern racket industry, where head-heavy rackets are marketed to aggressive smashing players which are supposed to give a higher shuttle velocity and head-light rackets are more manoeuvrable giving higher control and a better chance to defend against hard smashes.

2.4 Finite Element Method

The Finite Element Method, FEM, is a numerical method commonly used to solve engineering problems. A model representing a physical geometry is divided into a finite amount of elements, a mesh. By putting this model in a simulation environment the model behaviour is evaluated. This is done by calculating how the applied load and boundary conditions affects each element. The resolution and reliability of the FE-model partly depends on the number elements and how they are organised. In most cases, but not all, a finer mesh gives a more precise result and facilitate iterative calculations, however the computational cost increase as the time to finish a simulation increases. A case where finer mesh gives a less reliable result is where the elements are smaller but organised so that the quality of the mesh is reduced.

2.4.1 Mesh

The quality of a mesh can be defined in several ways, one part is to evaluate the geometric shapes of the elements and compare them to the ideal shape. Together with mesh convergence studies and other benchmarking aspects as element formulations and adaptiveness etc., the quality can be defined. It is needed to have reliable results. By knowing the most weak sections in the model regarding element quality the user is able to pick the areas used for data extraction more carefully.

For the element shape, some of the more common parameters are aspect, skewness and warping for each included element. Figure 2.4 to 2.6 illustrate schematic pictures of how the quality regarding aspect, skewness and warping are calculated for shell elements in Ansa. The aspect is a measurement of how equal the length and height are for triangular and quadrilateral elements, whereas skewness defines how far the element deviates from an equilateral triangle and quadrilateral. Regarding the warping angle, it is calculated by using the node distance h in Figure 2.6 which is calculated from the middle plane corresponding to the ideal orientation of the element, i.e. with the nodes orientated in the same 2D-plane.

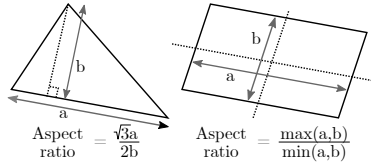


Figure 2.4: Definition of shell element aspect according to the Patran criteria in Ansa.

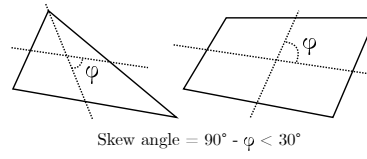


Figure 2.5: Definition of shell element skewness according to the Patran criteria in Ansa.

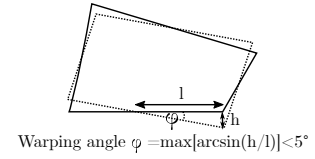


Figure 2.6: Definition of shell element warping according to the Patran criteria in Ansa.

The quality parameters are calculated slightly different for solid elements, see Figures 2.7 and 2.8. For the hexa elements, a brick element of first order which has an equivalent shape of a cube and is defined using 6 faces and 8 nodes, Ansa check each surface for warping using the same definition as for shell elements. The surface which performs worst regarding the warping criterion define the number assigned to the volume element. The aspect is measured similar to the shell element formulation although as another dimension is included the min and max length is used to calculate the worst aspect. Finally the shape factor is used to determine the skewness where the volume of the perfect cube is compared to the volume of the element and for the perfect shape the factor is equal to 1. In the figure 2.8 this is illustrated for tetrahedrons as the procedure is similar [21].

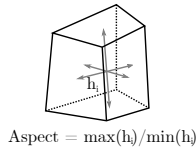


Figure 2.7: Definition of volume element aspect according to the Patran criteria in Ansa.

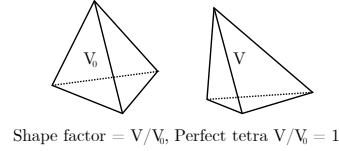


Figure 2.8: Definition of volume element skewness according to the Ansys criteria in Ansa.

2.4.2 Hourglass

The finite element discretisation is based on assumptions and simplifications which introduces minor errors that can be negligible or serious depending on whether the assumptions are valid or not. One important behaviour is the hourglass effect for elements using reduced integration. For shell elements this is when an element is used with only one integration point in the shell plane. A reduced shell element has five hourglass modes which all are a form of un-physical deformation occurring in the FE-model due to the lack of integration points. These modes are so called zero energy modes which imply that they can be triggered without any use of strain energy. Figure 2.9 illustrate the effect from hourglassing for a shell mesh. As can be reviewed the mesh has a distorted deformation which is non-physical.

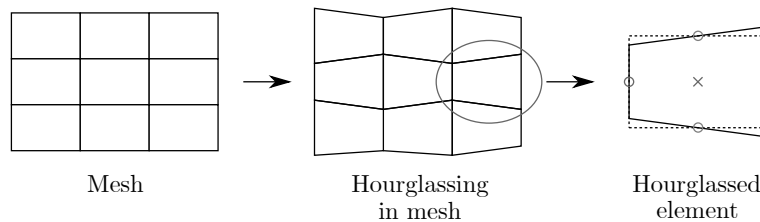


Figure 2.9: The effect of hourglassing in a 2D shell mesh.

By using fully integrated elements, this unwanted behaviour would be prevented. But using fully integrated elements is time consuming. Hence, in many cases hourglassing is allowed but controlled using various methods to artificially add the energy corresponding to an hourglass mode. These energies acts as nodal counter forces preventing the unwanted deformations [22].

2.4.3 Elements

When using the software LS-Dyna for a model consisting of shell elements the standard type of element is Belytschko-Tsay element (Element type 2). The element is based on the kinematic relation of Mindlin-Reissner theory where plane stress is assumed. Comparing to the more simple theory of a Kirchhoff plate, the shear strains are considered. This is analogous to the Timoschenko beam theory illustrated in Figure 2.10 where the deformation is explained by mid plane displacement w and the rotation θ giving the shear strains. The cross section still have the initial linear shape but can be rotated around the point located on the mid plane. For Kirchhoff plate theory the through thickness deformation is perpendicular to the mid surface, thus no shear strains are captured [23].

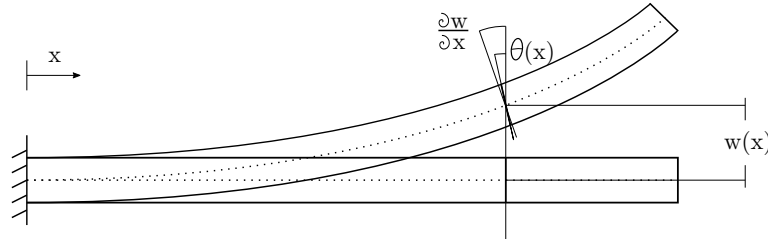


Figure 2.10: *The kinematic assumption for a Timoschenko beam.*

The element is reduced using one in-plane integration point, see an illustration in Figure 2.11, meaning that it is computational fast but introduce the risk of hourglassing. Thus, this behaviour needs to be controlled when using reduced elements. An error check using fully integrated elements for a similar model could be needed to control the difference in the results between a mesh of reduced and fully integrated elements to satisfy a good accuracy. Further, by using the Belytschko-Tsay formulation the quality of the mesh may influence the result and cause unreliable results. Thus, it is important that correct limits for the quality is defined in a proper way, especially for warping [23]. For shell elements, Stelzmann recommend only one other type of element and that is the fully integrated shell element formulation using 2x2 integration points in the shell plane. The formulation prevent the existence of hourglassing modes but its downside is a more expensive calculation with an increase around a factor of 2-2.5. The formulation does not completely resolve the problem with warping but this can be countered by using hourglass control with the parameter *IHQ* set to 8 in LS-Dyna, although it gives an even more expensive calculation in terms of time [24].

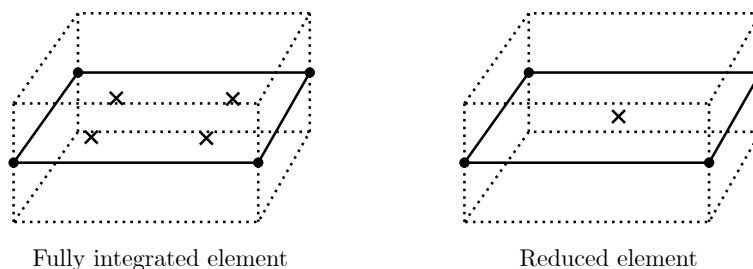
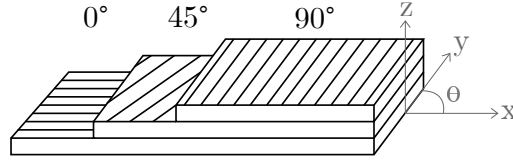


Figure 2.11: *Illustration of a fully integrated element and the corresponding reduced element.*

2.5 Composite Mechanics

A composite material consists of fibres and a matrix holding these fibres in place. Thus, the properties of a specific composite material is determined by the amount and characteristics of these two parts. A unidirectional-ply (UD-ply) is a sheet with fibres aligned in the same direction. Thus, a layer of composites are modelled using a combination of UD-ply where the fibres are orientated different for each layer. In Figure 2.12, an example is given where the orientation offset is based on the x-axis meaning that 0° is along the x-axis while 90° is perpendicular. A notation commonly used in fibre composites is index L for the direction along the fibres and T for the transversely direction, i.e. L-direction in the figure for the first ply is along the x-axis while for the 90° ply it is along the y-axis.

Figure 2.12: *Composite Layup and Orientation.*

Because of the schematics of the composites with fibres orientated in different directions it is an orthotropic type of material, meaning that the material properties are directional. For linear elastic models of the material Hooke's law can be used to calculate the Cauchy stress under the assumption of small strains. Using index notation the equation is defined as:

$$\sigma_{ij} = E_{ijkl} \epsilon_{kl} \quad (2.1)$$

As the stress and strain tensors are symmetric they can be reduced to 6x1 vectors when using Voigt format. Moreover orthotropic materials have the same properties in the normal and reversed normal directions for certain planes. This means it has the same stiffness regardless if it is in compression or tension. Furthermore, for this project the composite plies were considered to be transversely isotropic meaning that the plane perpendicular to the fibre direction is isotropic, i.e the properties perpendicular to the longitudinal directions are the same regardless of orientation within the plane.

Given that the Young's modulus for the transversely and longitudinal directions are known, E_T and E_L , together with the major Poisson's ratio ν_{LT} then the minor Poisson's ratio ν_{TL} is given by [25]:

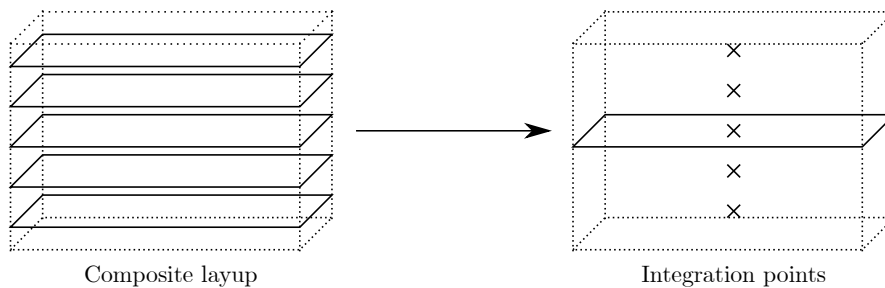
$$\nu_{TL} = \nu_{LT} \frac{E_T}{E_L} \quad (2.2)$$

Given that there exists a plane of isotropy the shear modulus for this plane can be calculated with Equation (2.3). It is rare to have all material parameters available and several of these parameters are fairly complicated to model as they require additional parameters to define. Nevertheless as stated in the Composite Mechanics course at Chalmers [26] the value of $\nu_{TT'}$ is normally in between 0.4 – 0.45 for some carbon-epoxy materials.

$$G_{TT'} = \frac{E_T}{2(1 + \nu_{TT'})} \quad (2.3)$$

2.5.1 FE-model of Composite Materials

A composite layup is a complex structure with plies stacked in different orientations and with different materials. Hence the FE-model require a proper definition of the composite to capture the correct behaviour. Regardless if shells or solids are used to model the composite layup, the option remains if each ply is to be model with a corresponding element or a through thickness integration point using only one element, see Figure 2.13. If efficiency is prioritised or only the elastic response is of interest, the integration points method is recommended to lower the computational time needed. The downside is that delamination will not be captured properly as a contact condition needs to be defined between elements to obtain the separation behaviour [27].

Figure 2.13: *FE-model of composite materials.*

2.6 Motion Capture

Motion capture is a technique to capturing movements of people or objects using a sensor, typically a camera. It is used widely to capture physical movements and transfer them to computer animations. It has also become a standard tool in sports, where for example the Hawk-Eye system is used to help the referees make the correct calls in badminton games [28].

Motion capture has been used to capture the motion and behaviour of a badminton racket in previous badminton studies at Aalborg University [4] [29] [30]. These recordings were made using a system by Qualisys containing eight cameras recording at 500 Hz and saved to C3D, coordinate 3D, files. To follow the movement of the racket five markers were placed on the racket, see Figure 2.14. The position of these were recorded and compared to data from strain gauges positioned on the racket showing that the method gave reliable results.

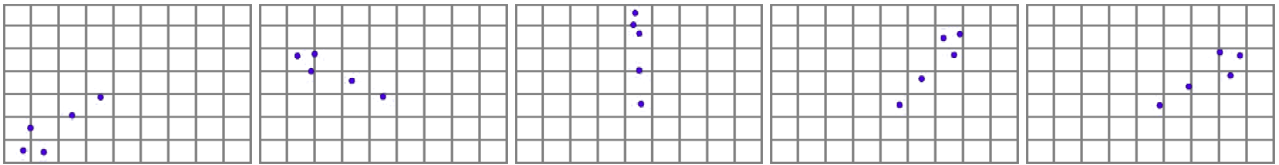


Figure 2.14: *A motion capture sequence with five markers on a badminton racket.*

3

Method

The objective of the study was to find how racket design parameters impact the performance of a badminton racket. A condensed view of the method can be seen in Figure 3.1.

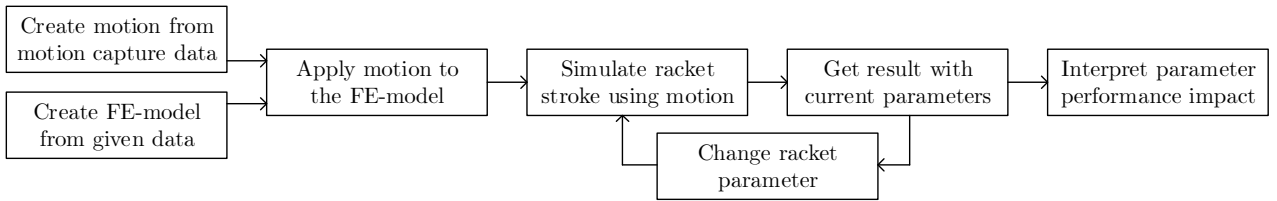


Figure 3.1: Overview of the method used in this study.

3.1 Used Software Products

To create the model and process the results in this study several computer software were used. The usage of these are detailed below and are shown in the flow chart of Figure 3.2.

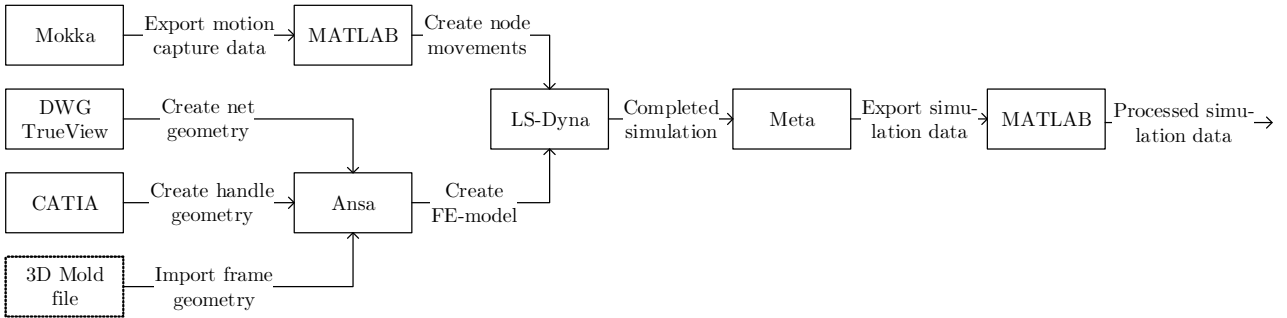


Figure 3.2: Overview of the usage of software.

Mokka An open-source software which can be used to analyse motion capture data C3D files. Was used to export the motion data to a comma-separated value format which was processed in Matlab.

MATLAB A commercial software used for numerical computations. Was used to processes the motion data and to process the data simulation results outputted from Meta.

DWG TrueView A free software used for looking at CAD, computer aided design, drawings. Was used to accurately reproduce the net geometry from the drawing.

CATIA A commercial software used for CAD. Was used to create the handle geometry.

Ansa A commercial software used for pre-processing the FE-analysis. Was used to create the FE-model which was based upon the imported 3D geometries.

LS-Dyna A commercial software used for FE-analysis. Was used as the solver for the FE-problem.

Meta A commercial software used for post-processing the FE-analysis. Was used to export data from the simulations that ran in LS-Dyna. It is made by the same company that makes Ansa.

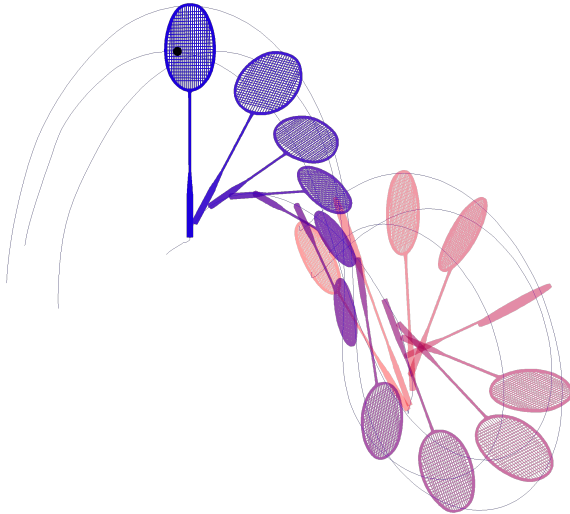


Figure 3.3: *Visualisation of the clear swing motion, going from red to blue as time increases.*

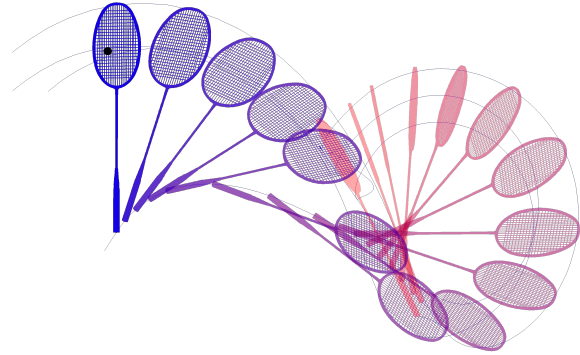


Figure 3.4: *Visualisation of the smash swing motion, going from red to blue as time increases.*

3.2 Racket Motion

The FE-simulation of a moving badminton racket required knowledge about the swing motion. This data had already been recorded in studies at Aalborg University. From these studies, data for two types of badminton strokes was provided: the clear (Figure 3.3) and the smash (Figure 3.4). It was recorded with the Qualisys system described in Section 2.6. The look of the two swings are very similar, where the major difference is found in the vertical movement of the clear swing. This is due to a restriction in the original smash study where the shoulder movement was kept to a minimum.

The movement data was exported from Mokka to a format readable in MATLAB. It contained xyz-position data for each marker on the racket, see Figure 3.5, during about one and a half second, where the swing motion was roughly 0.6 seconds long. This data was smoothed to remove small jitters in the data which most likely is due to error in the capture process, see Figures 3.7 and 3.8. By removal of the small fast movements, the FE-analysis became more stable and visually looked more like the movement of a swing. The movement was applied to the racket by controlling translation and rotation of the bottom node, see Figure 3.6.

The motion capture for the clear stroke also contained data for the post impact shuttle speed, which was almost 50 m/s right after impact.



Figure 3.5: *Markers used in the motion capture. Attached on the outside of the frame and handle.*

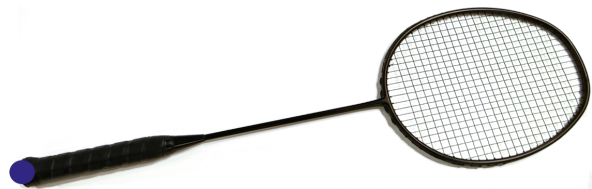


Figure 3.6: *Node used to control model movement. Positioned in the center of the handle bottom.*

3.3 CAD Model for the Racket

The finite element model was based on a provided 3D CAD model defining the geometry for the shaft and the head of the racket. Furthermore, a 2D blueprint was supplied with a definition of the stringed area. Regarding

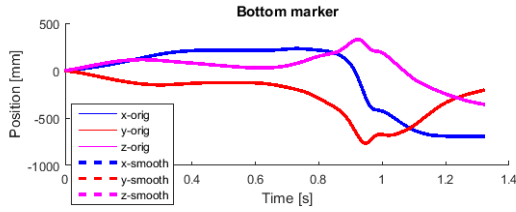


Figure 3.7: The xyz -position of bottom marker, original data and smoothed data (overlapping).

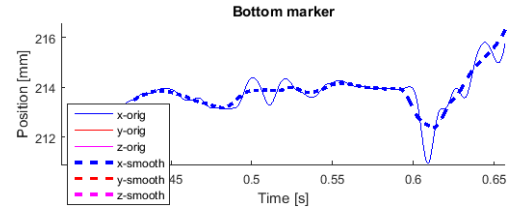


Figure 3.8: Original and smoothed x -position data, zoomed in.

the handle no schematic definition was given. Also supplied were three different physical prototypes, all with the same geometry but different material layup. This geometry and chosen material properties defined the original model, thus changes in responses due to parameter alternations were evaluated against this model.

3.3.1 CAD Model for the Head and the Shaft

In Figure 3.9 the CAD model for the original model, an isometric shaped racket, is illustrated. This CAD-model, which was given by Salming, was possible to import into Ansa. It is the part where alterations were made to evaluate the different geometrical influences in the parametric study.

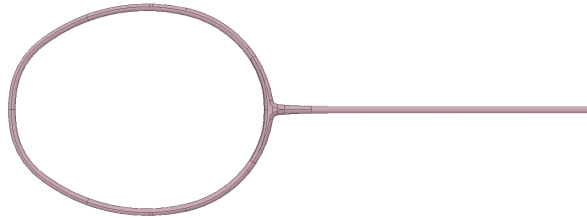


Figure 3.9: CAD model of the frame.

3.3.2 CAD Model for the Net

The geometry of the net was added to the frame in Ansa using a 2D-drawing defining the stringed area, see Figure 3.10. Here a small error was revealed as the drawing include one more horizontal string than the psychical model. The strings were chosen to be based on the drawing as this was easiest and the racket was already deviating from the prototypes due to lack of material data. The string bed consists of 22 vertical and 23 horizontal string sections. The strings had a diameter of 1 mm giving it an cross sectional area of 0.72 mm^2 .

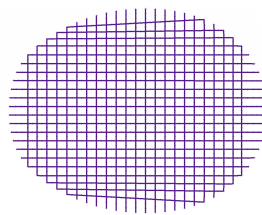


Figure 3.10: The resulting stringed geometry, taken from the 2D-drawing.

3.3.3 CAD Model for the Handle

For the handle, see Figure 3.11, as mentioned above no schematics were accessible. Thereby, the geometry was estimated by measurements. The handle is a stiff volume with the purpose to provide the player with an firm and controlling grip. The shape is optimised to suit the hand with a low weight. The bottom half of the handle is hollow reducing the weight contribution to the racket. Furthermore the handle has a plastic plug at the bottom and a plastic cone that is glued across the cone-shaped surface of the handle. These were neglected in

the project due to the lack of material data and presumably their influence on the elastic behaviour of the racket is negligible.

Furthermore, to obtain a good grip the handle surface is covered with a grip tape. This part was excluded for this project as it was assumed to have little impact on the structural responses of the racket. As the hand was not accounted for in the FEM model, there was no reason for the grip tape to be included which otherwise would damp the vibrations transferred into the hand.



Figure 3.11: *CAD model of the handle.*

3.3.4 CAD Model for the Shuttle

As the simulations including the shuttle only considered the small window before and after hit, the aerodynamics of the ball was neglected. Thus, the otherwise complex geometry of the shuttle is simplified to a ball, see Figure 3.12. This model had the same radius as the cork part of the shuttle with an equal weight. With other words no CAD model was provided and the ball was created directly in Ansa.

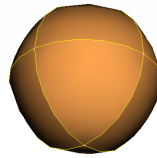


Figure 3.12: *CAD model of the simplified shuttle.*

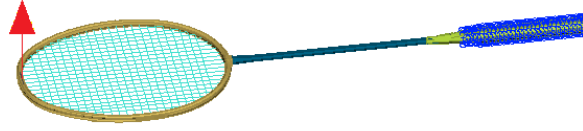
3.4 Material Properties

The modern badminton racket consists of several different materials. The frame, handle, strings and other small components are all made of different materials that is carefully chosen to be the optimal material for each parts purpose. To fully capture the true model response it was important to model the materials with the right properties. Even though several different prototypes with varying material composition was provided by Salming, no material data was known. Hence, the project focused on a general method for evaluation badminton racket, but due to the lack of data a full validation for the provided racket was not possible to achieve. To get realistic properties the material data was gathered from the material database CES Toolbox. Further, as it was of great importance to obtain a correct center of gravity for the racket the density presented below are not directly taken from CES but tweaked to fit the given prototype. The presented material properties following in this section defines the original model. Thus, if an evaluation of a 10% stiffer material was made it was with these values as reference.

3.4.1 Static Bending Test for Material Verification

Even though the total weight and its distribution was modelled correctly, properties as damping and stiffness of the racket are equally important to capture the racket behaviour properly. A theory of why badminton is such a high velocity ball sport is that it depends on the flex of the racket. Thus, the racket material behaviour regarding stiffness was calibrated using a simple bending test. The provided prototypes were evaluated for bending stiffness by clamping the handle and applying a load at the top of the racket upwards using a small baggage scale.

The result was then used as a reference when simulating the bending test for the FE-model with the chosen material. In Figure 3.13, the boundary condition for the simulations are illustrated with the clamped handle defined in blue and the applied load as the red arrow. The FE-model is described in detail in Section 3.5.

Figure 3.13: *Boundary condition for the static deflection test.*

3.4.2 Composite Material for Frame

When looking at advertisement and selling arguments for badminton rackets the main focus is usually on the shaft and frame. Different tweaks regarding stiffness and geometry is common and the properties of the badminton frame is frequently debated. It is visualised by the abundance of different layups and material compositions for the badminton racket hinting that it is hard to find the best design. Consequently, the main focus of the material evaluation revolve around the properties of the composite structure. The racket consists of two different composites structures, one for the head and one for the shaft. The head was modelled with a stiff material with the following properties:

$$E_L = 160 \text{ GPa} \quad E_T = 12 \text{ GPa} \quad G_{LT} = 7.1 \text{ GPa} \quad \rho = 900 \text{ kg/m}^3 \quad \nu_{LT} = 0.3$$

While the shaft was modelled with a less stiff material with the following properties:

$$E_L = 70 \text{ GPa} \quad E_T = 8.9 \text{ GPa} \quad G_{LT} = 7.1 \text{ GPa} \quad \rho = 1400 \text{ g/cm}^3 \quad \nu_{LT} = 0.3$$

Using Equations (2.2) and (2.3) with $\nu_{TT'} = 0.4$, the shear modulus and the minor Poisson's ration in the transverse isotropic plane was obtained. For the head material $\nu_{TL} = 0.0225$ and $G_{TT'} = 4.3 \text{ GPa}$ while the shaft material had $\nu_{TL} = 0.0384$ and $G_{TT'} = 3.2 \text{ GPa}$.

No method to measure the composite layup was available, hence a layup of 0 and 45 degree plies were chosen with the static test as a reference. Both the head and the shaft was defined with a layup of $(0/\pm 45/0)_S$, as a result from the calibration test, with a total of 8 plies. Further, the ply thickness for the shaft was set as 0.15 mm and for the head 0.225 mm.

3.4.3 Wood Material for Handle

According to Salming, attempt has been made with handles consisting of carbon fibre. The reason why to this point these rackets is rejected by many players is due to the harsh vibrations that come with the carbon fibre handle. The material used for the handle was therefore chosen to be wood as it is the current standard. The following properties was used:

$$E = 20 \text{ GPa} \quad \rho = 720 \text{ kg/m}^3 \quad \nu = 0.3$$

3.4.4 Material for Strings

Just as for the racket frame, there are an abundance of different choices regarding strings. As the strings influence was beyond the scope of the project the material properties were fixed for all simulated models with the exception of the density which was altered for some models when the mass was modified. The strings were modelled with the properties of Nylon:

$$E = 23 \text{ GPa} \quad \rho = 800 \text{ kg/m}^3 \quad \nu = 0.3$$

3.4.5 Cork Material for Shuttle

Due to the simplification of the shuttle, the feather or synthetic material was neglected and only the cork material was modelled. Regarding the Poisson's ration there was a large interval for the value in CES varying between 0.05-0.45 i.e. from almost fully compressible to incompressible. According to Silva et al., due to the

structure of the cork material, the cell walls building the cork structure will fold when compressed. Consequently cells are not expanding in other directions and the resulting behaviour is that the material are close to fully compressible with a small Poisson's ration [31]. Another way to illustrate this is by simply evaluate a glass bottle with a stopper made of cork, a wine bottle for instance. The cork do not bend above the edge of the bottle even if it have been compressed to fit the bottleneck, which further verifies the compressibility. The following values for the cork material were used:

$$E = 30 \text{ MPa}$$

$$\rho = 700 \text{ kg/m}^3$$

$$\nu = 0.05$$

3.5 The Finite Element Model of the Racket

The following section describes the procedure used to model the racket prior to the simulation. Using the graphical interface in Ansa the FE-models were defined, suitable for the LS-Dyna environment, both when it comes to the computational domain but also the racket response when exposed to the swing simulation.

3.5.1 Defining Part Identities (PID)

The CAD files for the frame and handle was loaded as stl-files and assembled in Ansa. As mentioned in Sections 3.3.2 and 3.3.4, the net and the shuttle had no 3D geometry given and where directly defined in Ansa. Due to the fact that the different parts and sections of the model required different mesh procedure, both in terms of element type and form, the domain was divided into different properties with belonging part identification (PID) and color. In Figure 3.14, an illustration of the distribution of PIDs can be reviewed and the definition of each PID is listed in Figure 3.15. Not only did the PID definition facilitate the meshing procedure, it also provided more options when boundary conditions were defined together with material definitions. For instance, one parameter to evaluate was to vary the center of mass which easily was done assigning the assigned PID materials different densities.

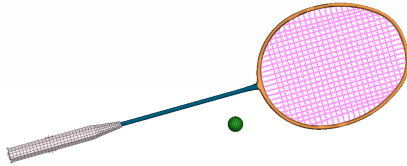


Figure 3.14: Part definition by color in Ansa.





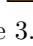
	Id	Name	T1	PID
	1	Shaft		1
	2	Net		2
	3	Handle		3
	4	Shuttle		4
	5	Frame		5

Figure 3.15: List of PIDs in Ansa.

3.5.2 Meshing Procedure and Used Element Formulations

A combination of solid, shell and truss elements was used to create a mesh of the racket. The wooden handle was modelled using first order shell elements with node based thickness.

The shuttle was modelled with solid elements using the hexablock meshing procedure in Ansa. The advantage with this method is that the mesh structure can be controlled simply by alter the controlling boxes. Further the geometry was copied well without the use of tetrahedron or pyramid elements which both are less accurate types of elements.

The head and shaft consists of composite material with a hollow structure with a constant wall thickness for each part. Further, the composite was modelled using first order shell elements with one element in the thickness direction. Thus, the layup was modelled using integration points for each composite ply. Furthermore, the shell elements were of reduced type to prioritise the efficiency.

Finally the net was meshed with truss elements, a two node element that only support axial loading i.e. only translation DOFs are defined. The reason for using truss elements was based on the characteristics of the strings which, without tension, only provide support to axial tension. Further different attempts were made to introduce a pretension into the strings and the most simple way in LS-Dyna was to add the pretension using dynamic stress relaxation defined in the truss element card, which was another argument to use that element

formulation. In total, the number of elements was 4167. In Table 3.1 the type and number of elements are listed in detail for each PID. A mesh convergence study was done to evaluate the accuracy and the results are presented in Section 4.3.

Part	Element shape	Type of Element	Number of Elements
Handle	Quadratic	Belytschko-Tsay(Reduced)	368
Handle	Triangular	Belytschko-Tsay(Reduced)	19
Shaft	Quadratic	Belytschko-Tsay(Reduced)	360
Shaft	Triangular	Belytschko-Tsay(Reduced)	1
Frame	Quadratic	Belytschko-Tsay(Reduced)	1340
Frame	Triangular	Belytschko-Tsay(Reduced)	19
Net	2D-bar	Truss	1844
Ball	Hexahedon	Fully integrated, 8 node with rotations.	216
Total number of elements			4167

Table 3.1: Table with detailed information of the elements included in the meshed domain.

The quality of the mesh regarding shape of the elements was measured using the parameters aspect, skewness and warping. Besides pure quality parameters, a minimum length was defined to prevent to large amounts of time steps and elements in the explicit simulation and also to prevent using very small elements close to larger ones. Table 3.2 consists of the limiting values for the quality of the mesh. Regarding aspect, the ideal case would be to have the value 1 which is also true for the warping when calculation for solid elements. For the skewness and shell warping angle the ideal value would be 0.

Type of Element	Quality param.	Value
Shell	Aspect	3
-	Skewness	30°
-	Warping	7
-	Min. Length	1mm
Volume	Aspect	3
-	Skewness	0.5
-	Warping	10
-	Min. Length	1mm

Table 3.2: Table of the minimum values defining the limit for the mesh quality.

3.5.3 FE-model of the Badminton Racket

Having a defined computational domain the properties of the model could be defined. Both in term boundary condition and contact behaviours and also part specific properties such as material and pre-stresses.

Consistent Units

One of the more important settings for the model was to ensure that the units were correctly defined and used in a proper way. That would otherwise lead to big flaws in the results from the simulations. For this project, the model was defined using the metric system with the units ms, MPa, mm, N and g. As a reference steel is defined by LS-Dyna support for each type of unit combinations with $\rho = 7.83 \cdot 10^{-3}$ and $E = 2.07 \cdot 10^5$, i.e. every material used in the model need to have the density and Young's modulus defined in the same manner [32].

Material Definition

The material in the FE-model was defined using two different material cards in LS-Dyna. For the solid parts and the net, an elastic material was modelled using the material MAT01 in LS-Dyna in which Youngs modulus, density and Poisson's ratio were defined. For the more complex composite material MAT116 for composite layup was used in which the different orthotropic properties were defined.

This means that the material has different properties depending on orientation and consequently the material definition regarding orientation was crucial to model the composites correctly. For the shaft this meant that the direction of the longitudinal fibres was aligned with the shaft axis, see Figure 3.16, whereas for the head the orientation was set to be tangential to the inner oval circle defining the head shape of the racket, see Figure 3.17. To ensure that this orientation updated properly, i.e. following the deformation of the racket, invariant node numbering was used [27].

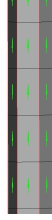


Figure 3.16: *Definition of material orientation for the shaft.*

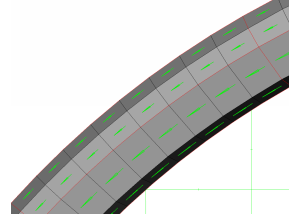


Figure 3.17: *Definition of material orientation for the head.*

Properties Card and Element Type in LS-dyna

As mentioned in Section 2.5.1 there are several ways of model a composite layup. To avoid the need of user defined integration rules and part specific definitions for each layer the *PART_COMPOSITE option in LS-DYNA was used. The part environment gives a simple overview of properties for the layup regarding orientation, thickness, material and identification for each ply. The total amount of integration points and thickness of the elements included in the part are the sum of all entries [33].

Due to the extent of elements available in LS-Dyna the selection of elements used for the model was based on results from a previous thesis [34]. In a bench marking study of steel-composite structures, Andersson and Larsson [34] tested the efficiency and accuracy for the most recommended element formulations by performing a simulation test of a bending cantilever. For shell elements, the fully integrated element had almost twice the calculation time compared to the reduced element but with similar accuracy comparing to an analytic result. Hence, the reduced element was recommended and was also the one used for this project with an hourglass formulation to prevent hourglass modes.

According to their test, using the reduced constant stress elements (ELFORM 1) an significant overestimation of the stiffness was obtained while the fully integrated elements (ELFORM 3) followed the analytic behaviour better. Thus the fully integrated element was recommended and even though bending will be a minor behaviour regarding the shuttle model this was the formulation used in this parametric study as well [34].

Damping

The damping was modelled based on the eigenfrequencies, f , of the model. Using the knowledge from the eigenfrequency simulations, a frequency range which included the lowest eigenfrequencies was set for which the vibrations was damped. LS-Dyna recommend that using this procedure the ratio f_{max}/f_{min} should not exceed 300, thus the limit for this ratio was set with a margin to 250 for this project. Further this approach will slightly decrease the dynamic stiffness of the model. But since this error was similar for all models no increase of stiffness was made as it was the relative value between the models that were interesting. The damping ratio, which is defined as the fraction of critical damping, was set to 0.02. LS-Dyna recommend that no ratios equal or higher than 0.05 should be used for this type of damping [33].

Boundary Conditions - Motion

The main objective for the FE-model was to capture the behaviour of the racket when swung in different badminton strokes. To enable the model to follow the motions given from the motion capture, the lowest nodes of the handle were defined as rigid with a rigid connection to an extra node placed in the middle, see Figure 3.18. This made it possible for the model to capture all motions including translations and rotations. This approach introduce local stress concentrations around the rigid nodes but since the results gathered from the simulations only consists of the elastic response with the stress distribution falling outside the scope, this does not affect the sought results. Further, the applied motions were placed far from areas that were of interest to evaluate.

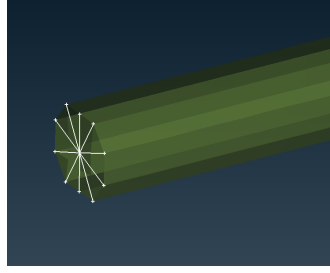


Figure 3.18: *Illustration of the nodes controlling the prescribed motion.*

The controlling node was prescribed in the translational and rotational degrees of freedom using the interpolated data for the motion capture data. By defining the curves controlling the prescribed motions as a separate file that was included in the model it was possible to, with ease, switch to different motions without any further alternations.

Regarding the shuttle no motion or boundary condition was applied at start but the possibility was left open to move the ball using the restart environment in LS-Dyna. By defining the card `*DEFORMABLE_TO_RIGID` the shuttle could be altered between being rigid and deformable to prevent any internal stresses and deformation to be introduced when the ball was to be moved into position before impact. As the ball was supposed to be hit with different orientations when simulating the strokes these features were desired preventing the shuttle to move away from the expected location when releasing the boundary condition.

Contact

Due to the different included parts there were several connections needed to be defined. The different parts of the racket had to be coupled with contact conditions but also the ball to net contact needed a definition. For the contact between the net and the frame it was assumed to be a tied contact between the inner frame surface and the most outer nodes for the net, i.e. there was no sliding between these parts. A fairly accurate assumption as the net in reality is strung in small holes around the frame. The only slide possible in the physical model was in and out of the hole, this will not alter the distance between each part of the net. Further, the contact between the shaft and the handle was modelled with three connections, which is illustrated in Figure 3.19, preventing the shaft to slide out from the handle. This way, the force will be transferred in the top connection creating a stress concentration assumed to leave the interested results unaffected.

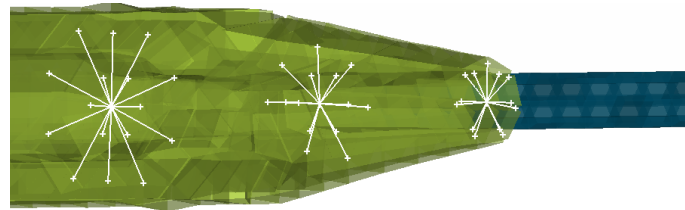


Figure 3.19: *Illustration of the nodes defining the contact between shaft and handle.*

Pretension of the Strings

As mentioned in Section 3.5.2 when the strings are attached to a badminton racket they are initialised with a pretension of 90-120 N depending on the player skill and requests. The racket in this project was modelled with a tension corresponding roughly 105 N, i.e. in the middle of the two extreme values. The truss element card in LS-Dyna model this is defined using a dynamic relaxation of the stress in the strings, i.e. a pre-stress of 140 MPa was introduced in the model.

3.5.4 Alternations for Model Used in the Implicit Eigenmode Analysis

Apart from the above defined FE-model, two others was used to capture some other behaviours that were needed for the interpretation of the simulated results. The first one was the model used to calculate the eigenmodes for the a clamped racket. All boundary conditions were removed, except the clamped bottom of the handle, including the shuttle and belonging contact definitions. Further, the damping was removed as it was unnecessary since the eigenvalues was calculated using an implicit static simulation. Apart from these simplifications the same pre-stress and material properties were used.

3.5.5 Alternations for Rigid FE-model

The third model was a rigid FE-model for the racket with the purpose to capture the motion behaviour for troubleshooting but also as a reference when analysis the deflection data. The model was made rigid using the LS-Dyna material MAT20 for all parts. To be able to control the time step in the simulation, one element separated from the racket model was defined with an elastic material as LS-Dyna is unable to define the time step using MAT20. This was defined with the element length of 7 mm, Young's modulus of 210 GPa, a viscosity of 0.3 and the density of 115 kg/m^3 giving a time step of $4.46 \cdot 10^{-3} \text{ ms}$. The contacts between the different racket sections were defined using rigid connections leading to a racket that moves as one rigid body.

When prescribed a motion for a rigid body in LS-Dyna, the rotations are defined around the coordinate system for the center of gravity of the affected part. To get around this a small controlling sphere, see Figure 3.20 was created in the bottom of the handle with the middle point coinciding with the controlling node for the deformable model. By setting a heavy weight for the sphere and a low weight for the rigid racket, the combined rigid body had a center of gravity in the center of the sphere. The boundary conditions were then defined on this sphere resulting in the same reference system as for the deformable model. Hence, the same motions are applied for the rigid model as for the deformable model.

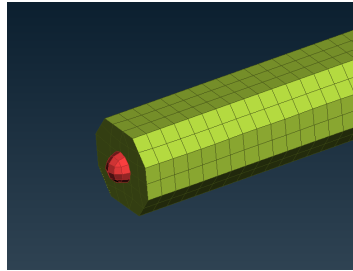


Figure 3.20: *Illustration of controlling ball for rigid model.*

3.6 Parameter Study

To find the impact of the design parameters of the racket, several models were analysed in the parameter study, see Table 3.3. The chosen parameters in the study were taken from conclusions in previous studies. These are:

- Head shape
- Center of gravity
- Weight
- Shaft stiffness
- Head stiffness

The models in the study are the original racket, which is based on a typical modern isometric racket with data from the bending test, and modifications upon it. Each modification focuses on one parameter being altered while keeping the other as in the original model. This isolation of parameter change was done to isolate the impact it has on the racket performance. For all parameters, excepted shape, the change was both to a greater and a lesser value. A greater value of centre of gravity was defined to as the point moving closer to the

Model	Head shape	Center of gravity*	Weight	Shaft stiffness	Head stiffness
Original	Isometric	301.1mm	84.4g	70 GPa	160 GPa
Stiff shaft	Isometric	± 0	± 0	98 GPa	± 0
Weak shaft	Isometric	± 0	± 0	42 GPa	± 0
Stiff head	Isometric	± 0	± 0	± 0	224 GPa
Weak head	Isometric	± 0	± 0	± 0	96 GPa
High CoG	Isometric	331.8mm	± 0	± 0	± 0
Low CoG	Isometric	270.2mm	± 0	± 0	± 0
High mass	Isometric	± 0	93.3g	± 0	± 0
Low mass	Isometric	± 0	76.3g	± 0	± 0
Prince	Y-shaped	± 0	± 0	± 0	± 0
Oval	Oval	± 0	± 0	± 0	± 0

Table 3.3: The racket models which were simulated and their parameter values. When shown ± 0 this means no deviation from the Original model. *from bottom of racket.

head and further away from the shaft. The head shapes chosen are the ones described in Section 2.2: isometric, y-shaped and oval.

The parameters were altered within different intervals. For the centre of gravity initial simulations showed that small alternations gave large differences. Thus, the interval was set as 10% lower or higher than the original position. The weight for existing rackets varies within small ranges. Consequently, the evaluated interval was defined as 10% lower or higher than the original. For the shaft stiffness initial simulations indicated that a higher variation was needed. Thus, the head and the shaft stiffness was evaluated for values 40% higher and lower than the original Young's modulus.

3.7 Simulations

The defined models were exposed to different simulations to obtain the necessary data for the parametric study. The simulations are defined over a specified time domain, thus the used time step required a definition. Each simulation explained in this section had a specific purpose as the combination of these defines the foundation on which the characteristics of a badminton racket could be defined.

3.7.1 Simulation Settings

The simulations were calculated using an explicit method due to the dynamic environment of a badminton stroke. The time step for the simulations was governed by the wave propagation in an element according to Equation (3.1), where l denotes the minimum element length for each element.

$$\Delta t_{min} = \frac{l}{c} \quad (3.1)$$

The parameter c corresponds to the wave propagation in a 3D-continuum, denoted c_s in Equation (3.2) or the speed of sound in the material which is calculated as c_t in Equation (3.2). Which c that LS-Dyna use depends on the effected element. For solids and shell elements, the value c_s is used whereas for the truss elements, the value c_t is used.

$$c_s = \sqrt{\frac{E(1-\nu)}{(1+\nu)(1-2\nu)\rho}} \quad c_t = \sqrt{\frac{E}{\rho}} \quad (3.2)$$

Consequently, the time step for each simulation was controlled by a single element, i.e. the smallest element that had the lowest stiffness and the highest density or the worst combination of these gives the lowest time step. With other words, to reduce the simulation time the smallest element was needed to be scaled up or the material properties had to be changed. Due to this limitation, a slight change in the time step was expected for the simulations where the model used different shapes that could lead to smaller elements or the models with alternated material properties.

As the models were using large amounts of time steps, well above 300 000, it was recommended to use double precision in the simulations to prevent round-off deviations. Even if the errors for each time step were extremely low, the amount of steps could lead to misleading results. In terms of simulation time this adds about 30 % which was considered to be an accepted amount for a greater accuracy. No mass scaling was used as even small mass differences could influence the result noticeably. The data, including deformations, accelerations, forces etc., was sampled with a frequency of 100 times per millisecond and the states which later were evaluated in Meta were sampled ones every other millisecond.

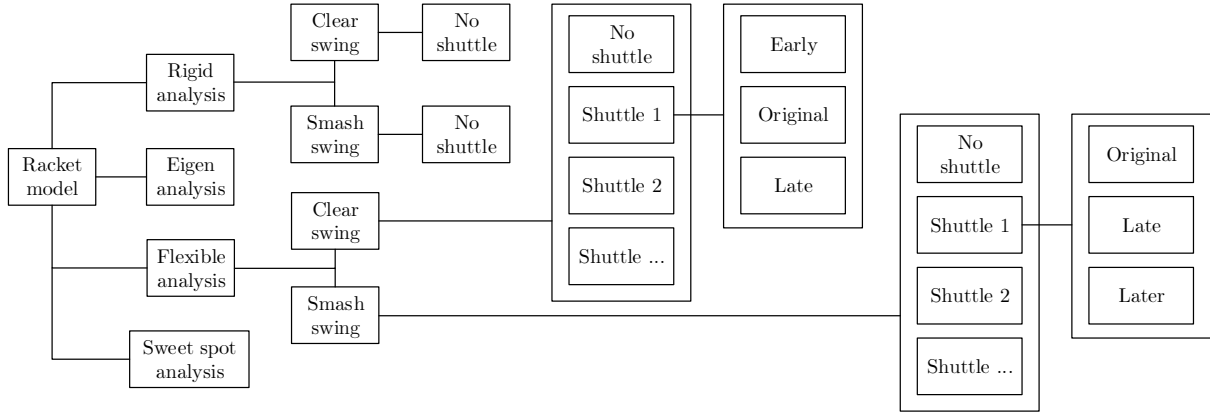


Figure 3.21: The simulations which are run for each racket model.

3.7.2 Execute Simulation

For each racket model several simulations were run. These consisted of an eigenfrequency analysis, a rigid body analysis and a flexible body analysis. The rigid body analysis was simulated twice using two different swing patterns and the same was done for the flexible body, which in addition to the normal swing also simulated 7 shuttle impacts. Additional sweet spot analysis and changed impact timing of shuttle 1 was also performed, see Figure 3.21.

The normal swing simulation and the shuttle impact simulation are identical up to the time when the racket strikes the shuttle. The time needed to run the several impacts could hence be greatly reduced by using the information from the normal swing. The normal simulation was run until 10 ms before impact where it was stopped and a restart file was created, which enables the simulation to restart from that state. This information was stored to be used for running each ball simulation. The normal simulation was then started from the restart state and ran until finished.

To simulate the impact between the shuttle and racket the shuttle needed to be positioned. The time between the restart state and impact was used to move the shuttle into position, without introducing any stresses to it. This means that all flexible body simulations did contain the shuttle and that the normal simulation intentionally missed it.

3.7.3 Eigenfrequency Analysis

The modal response for the racket was obtained by an eigenfrequency analysis. The different modes oscillates at different frequencies. During for instance a hit the experienced response is a combination of these modes. Furthermore, each mode has an individual shape which was evaluated to fully understand the influence of the vibration regarding the subjective feeling when using the racket.

Li et al. [35] suggest that for tennis rackets it is preferential to design with the target to obtain the lowest bending mode which include the highest amplitude and consequently the most amount of energy. Further it is showed that hitting a ball at the dead spot, i.e. where the lowest rebound effects are, give the peak in feedback for the player [35]. Hence, part of the players judgement on whether the stroke is performed correctly is governed by the vibrations of the racket. These studies indicate that eigenmodes is important to understand the characteristics of a racket, thus evaluating the influence from different parameters and how they affect the vibrations of the racket was desirable.

The simulation was done using the implicit solver. Based on the earlier mentioned FEM-model a simplified version was defined suitable for the implicit eigenmode analysis which is described in Section 3.5.4. The modal analysis was then performed on the clamped racket giving the vibrations of the racket.

3.7.4 Deflection Analysis

Badminton is said to be the fastest ball sport played and a part of the explanation of this is the deflecting behaviour of the shaft. Due to the slim design, the shaft deflects when accelerated. This phenomena creates a spring effect during the stroke which could lead to higher velocities of the ball. Thus, it was interesting to evaluate the deflection behaviour of the racket to see how the shuttle was effected for different flex.

For each type of stroke simulated the deflection analysis requires the full swing to analyse the deformation of the racket. Thus for each parameter, a total simulation of the stroke was needed. Consequently, the method for evaluating the parameters needed to be defined prior to the simulations to estimate the required calculation time needed to enable all simulations to be executed.

The method to obtain the deflections was to compare the deformable racket with a rigid model, i.e. for each swing and geometry a rigid model had to be simulated. However, the rigid model, consisting of the rigid material MAT22 in LS-Dyna, was much more time efficient to compute.

3.7.5 Sweet Spot Analysis for Swing

The velocity and path of the shuttle after a stroke largely depends on the string bed. The tension of the strings, geometry of the frame and the density of the strings are all parameters controlling the response from the stringed area, not to mention where on the stringed area the contact to the shuttle occurs. Thus, depending on the desired outcome when hitting the shuttle there could be different optimum characteristics of the strings. With this in mind the sweet spot of the simulated racket was analysed during the swing to predict the response for the different parameters. The sweet spot is defined as the area on the strings with the highest COR-value, calculated according to Equation 2.1.3. In Figure 3.24, a typical result from a sweet spot analysis is illustrated. The most yellow part shows the area where the COR-value is at its peak, i.e. this area is the sweet spot for this specific racket.

As illustrated in Figure 3.22, to capture the spread of the sweet spot the last part of the swing for each racket was simulated using different contact positions for the shuttle. With this setup the ball behaviour after hit was analysed by observing the velocity before and after hit together with the path of the shuttle.

One theory was that, as in a lot of sports, the contact time governs the amount of force that is transferred between the two object in contact. Thus, the contact time for the shuttle-to-strings contact was analysed for the different strokes and shuttle hits. By subtracting the rigid deformations and the deflections from the simulated stroke without any shuttle, the deflections due to the shuttle contact was obtained.

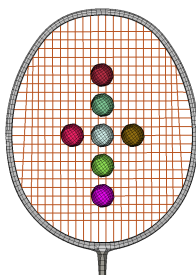


Figure 3.22: *Illustration of the distribution of the shuttle impacts for the swing.*

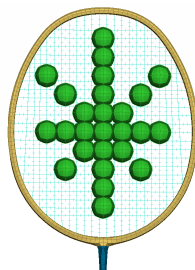


Figure 3.23: *Illustration of the shuttle distribution for sweet spot simulation.*

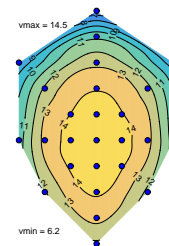


Figure 3.24: *A typical result of different rebounding velocities from the sweet spot analysis.*

3.7.6 Sweet Spot for Clamped Racket

To get a better resolution and understanding of the COR and re-bounce behaviour depending on impact location, another sweet spot analysis was made using a clamped racket without any applied motion. This simulation neglects the deformations otherwise occurring due to the swing. Thus, it gives a better picture of

the string bed behaviour if the racket is undeformed which is more realistic when including strokes with a much lower accelerations such as drop strokes.

In Figure 3.23, the distribution of the tested impact locations is illustrated using a total of 26 different locations. The simulations were done using all the different rackets and each simulation with a new ball is initialised with a impact speed of 20 m/s. The amount of simulations required to obtained the data was 286 st.

3.7.7 Time Window Analysis for Shuttle Impact

Due to the deflection behaviour of a badminton racket, if the results indicate that the deflection is affected by the different parametric alternations an additional simulation was of interest. By moving the ball backwards and forward in the path of the racket swing an earlier or later shuttle impact would be simulated. This would be done in a similar way as for the sweet spot analysis for the swing with restart files. Although the simulation was limited to the centred shuttle to minimise the amount of simulations. The time of impact and how the shuttle position should be changed was depending on the racket head velocity and the racket deflection as the peak values should influence the shuttle the most.

3.8 Method for Post-process and Organise Data

The parameter study generated a great amount of data which needed to be post-processed for the parametric impact. To prevent faults occurring from human errors during the post-processing a script was written and used. It ensured that the data was extracted from the study in the same way for each simulation. The data it extracted was:

- the position of specific points on the racket throughout the swing.
- the position of the ball center node, to capture the post-impact velocity.
- the data for the contact between the ball and the net, to get the amount of time of contact.
- the force applied to the controlling nodes, to find the force needed to swing the racket.
- images of the racket from the simulation.
- videos of the racket from the simulation.
- data and videos of the racket's eigenfrequencies and eigenmodes.

The chosen specific points on the racket can be seen in Figure 3.25. These are divided into three subdivisions: head, shaft and handle and given a name containing three letters for the shaft and five letters for the head and handle. For the head points, the first letter is *h* for head, the middle three indicating if positioned on top, middle or bottom of the head and the last letter if it is on the left, right or middle of the head width. The shaft uses a similar naming convention; *s* for shaft, then a number which incrementally grows with the distance from the handle and the last letter if on the left or right side. The handle uses the same type as the head, but the first letter was swapped to a *g* for grip to prevent confusion.

On the shaft and handle, the points are placed in pairs. This is to work around that the shaft and parts of the handle are hollow which means that there are no points and therefore no position data there. By having the node pairs a value for the virtual point between them can be positioned.

3.8.1 Post-processing Result in Meta

The software used to post-process the simulation results was Meta. It allows to record the actions used to post-process a result and can then repeat the same actions on other results. This was combined with Meta's Python API which allows the recorded actions to be combined with Python code into a batch script. The batch script was triggered to run when a new result was generated and extracted the wanted data. The data extracted by the Meta batch script was still too much to be handled manually. It was therefore imported into MATLAB to compare data and present it in figures and tables.

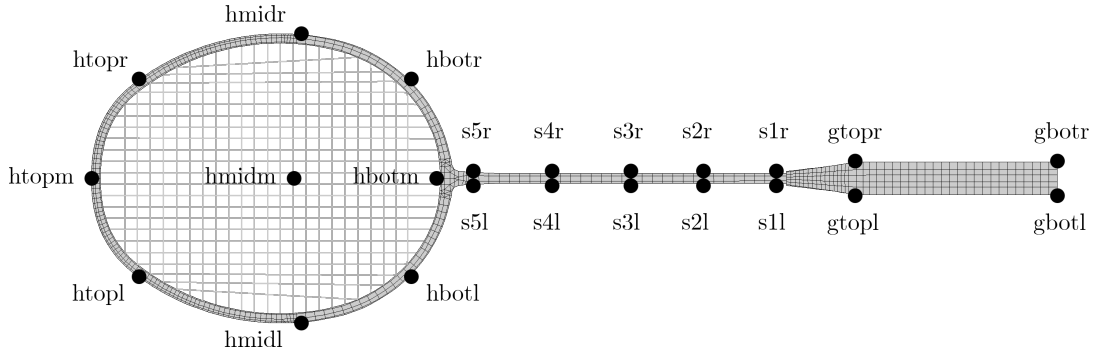


Figure 3.25: The points on the racket from which data was extracted in Meta.

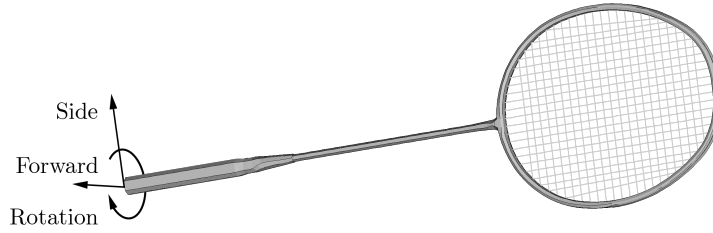


Figure 3.26: The coordinate system used to describe the deflection of the racket.

3.9 Post-processing in MATLAB

In MATLAB the final post-processing of the simulation results was made. The data put into MATLAB was:

- nodal positions of racket in rigid and flexible body simulation.
- shuttle position.
- force data for contact between shuttle and racket.

3.9.1 Comparison of Input and Output

The most essential result from the model was that it behaved similarly to the real racket. To evaluate this, the motion capture input data from the C3D files was compared to the node motion in the FE-simulation. The most interesting node to follow was the node at the top of the racket, as it is furthest away from the motion controlled bottom node.

3.9.2 Deflection of the Racket

The deflection of the racket in the simulation was defined as the difference in nodal position between the rigid and flexible model. As both models were swung using the same motion pattern, if the flexible body did not deflect it would perfectly co-inside with the rigid body. The deflection was calculated using three degrees of freedom: forward, side and rotational deflection, see Figure 3.26. Any deflection along the direction of the racket axis was neglected and seen as the result of the racket being bent forward or sideways.

The forward and sideways deflection were calculated by taking the vector result subtracting $\text{node}_{i,\text{rig}} - \text{node}_{i,\text{flex}}$ and then projecting it onto the forward and sideways directional vectors. The rotational deflection was only calculated for the head of the racket, which is where the greatest rotation would be found. This was done first by aligning the racket's rigid and flexible centre head nodes, $hmidm$, with each other. Then, by examining the angle between the vectors pointing to the rigid and flexible left side head nodes, $hmidl$, and the angle between the vectors pointing to the rigid and flexible right side head nodes, $hmidr$, two angles were found. These were then averaged, as they always were very similar, to get one value of the rotational deflection of the racket about its axis.

3.9.3 Shuttle Motion and Contact

Movement data for the shuttle was gathered from the simulation. This was used to find the speed and the trajectory of the shuttle. The angle of the trajectory was only measured in the horizontal plane, i.e. only looking how much to the left or right the shuttle went and disregarding upwards or downwards. This was done to make it easier to understand the difference in trajectory and as this was deemed to be the most crucial angle of error.

The trajectory was deemed to be straight, having 0° offset, when it followed the trajectory of shuttle 1 for each separate FE-model. This was used as it was hard to decide a true 0° offset, where knowledge would be needed of where the player in the recorded motion was actually aiming. The trajectory of the other shuttles, shuttle 2 - shuttle 7, are then evaluated against the trajectory of shuttle 1 to find the angular offset.

The information about the contact between shuttle and the racket was given by the contact force data, which was nonzero when there was contact.

3.9.4 Sweet Spot Analysis

For each racket 26 shuttle impacts were performed in the sweet spot analysis. The position data for the shuttle post impact was used to get the velocity of it. This was used to create a table containing the average, standard deviation, minimum and maximum value of the shuttle velocity for each racket model. The data was also used to create plots to create contour plots for the area within the outer ring of impact locations. To calculate the values between the data points the cubic interpolation technique inside MATLAB's `griddata` function was used.

4

Result

In this section the results from the simulations described in Section 3.7 are presented. The first part includes the validation for the global behaviour regarding motion and stiffness. Sequentially, the vibration behaviour for the different models are evaluated in terms of eigenfrequency. The two simulated strokes are evaluated for the different parameters and how these impact the performance separately. Throughout the report, the racket denoted original racket is defined as the reference racket. Hence, the alternations are measured against this racket. This means that the data in each table is the difference compared to the original racket and the absolute value given is for the original racket only. Absolute values for all racket simulations can be found in Appendix A, but as the FE-model was created without knowledge of the true material data only the relative impact of each parameter is considered.

4.1 Racket Motion

The applied motions were from two separate motion captures described in Section 3.2; one of a clear swing and one of a smash swing. The motion of the clear swing was relatively smooth and only minimal smoothing of the data was needed. The smash data was less smooth which resulted in some shakiness persisting in the applied swinging motion even after the data was smoothed. This noise in the smash movement produced vibrations in the racket frame mostly noticeable at low racket velocities furthest away from the applied motion, at the top. At higher racket velocities, i.e. at impact, the influence from the vibrations are negligible.

To find out if the movement in the FE-model did simulate the movement from the motion capture, the recorded movement of the top marker was compared to the top node's position data from the simulation of the original racket model. This data is shown in Figure 4.1 and Figure 4.2 for the clear and smash respectively.

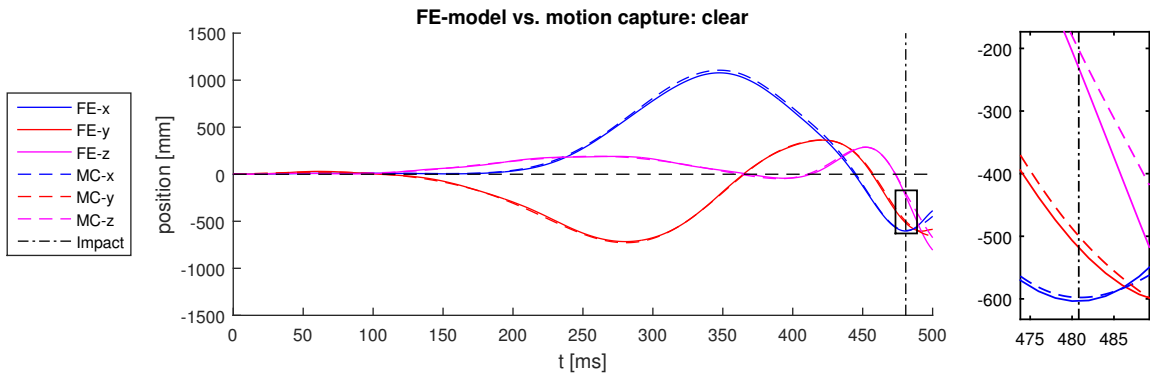


Figure 4.1: Comparison of C3D in-data vs. Meta results for clear swing.

The top node of the simulated original model follows the path given by the top node in the motion capture well in both swing motions, and crucially do not deviate significantly at impact. For both of the swings the motion capture data has a greater max position away from the starting position, a result of the motion data being measured outside the frame at the top of the head, see Figure 3.5, while the FE-model data is taken from within the frame, see Figure 3.25.

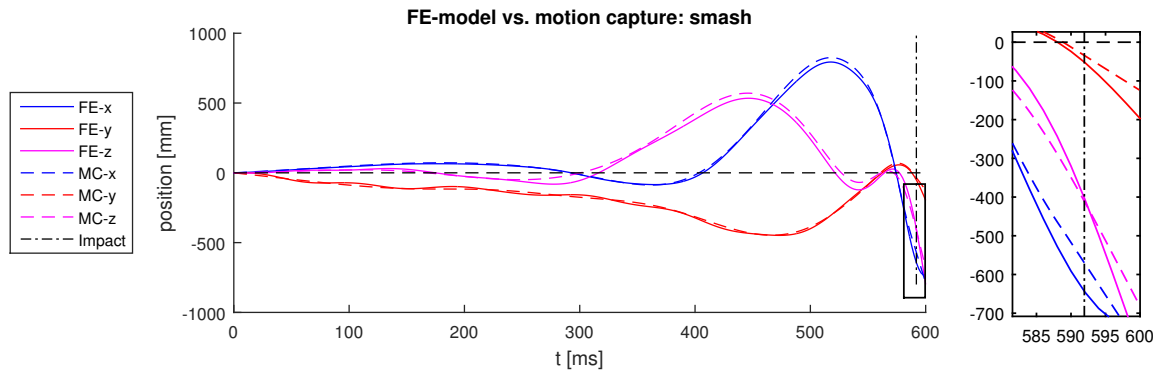


Figure 4.2: Comparison of C3D in-data vs. Meta results for smash swing.

4.2 Static Deflection Test

In the calibration tests, three different prototypes, with slightly different stiffness, provided by Salming were examined using the method described in Section 3.4.1. The top of the racket was subjected to a force which bent it upwards, see Figure 4.3. Each racket was subjected to the same magnitude of bending and in Table 4.1 the used force is presented. The combined average for all rackets was a force of 18.3 N needed to achieve the deflection of 110 mm.

	Deflection at top of racket	Average force
First Prototype	110 mm	18.1 N
Second Prototype	110 mm	19.3 N
Third Prototype	110 mm	17.5 N

Table 4.1: Experimental data for bending test.

In Figure 4.3 the simulated bending is illustrated using the FE-model. As presented in the picture the maximum tip displacement is 14.8mm which deviates from the experimental data with 3.8mm. Thus the FE-model model is slightly more flexible than the provided rackets prototypes in terms of forward/backwards deflection.

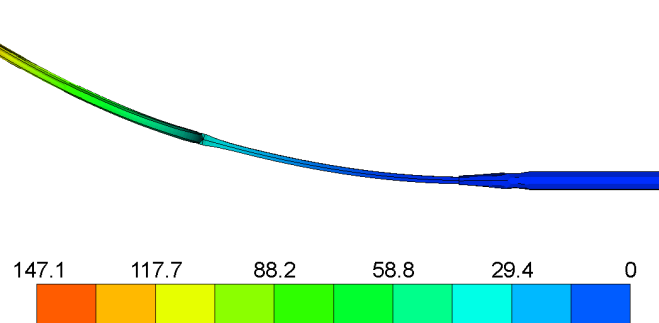


Figure 4.3: Deformation upwards from the static test for shaft bending, given in millimeters.

4.3 Mesh Convergence

In Figure 4.4, the top node displacement is presented for the original racket using different mesh. It can be seen that the mesh used to model the different rackets gives lower peaks within the interval of 180 ms - 480 ms. However the behaviour of the displacement is similar for all the different meshes. Furthermore, the maximum displacement was evaluated and the result is presented in Figure 4.5. No steady state is obtained although the difference is small within the evaluated interval.

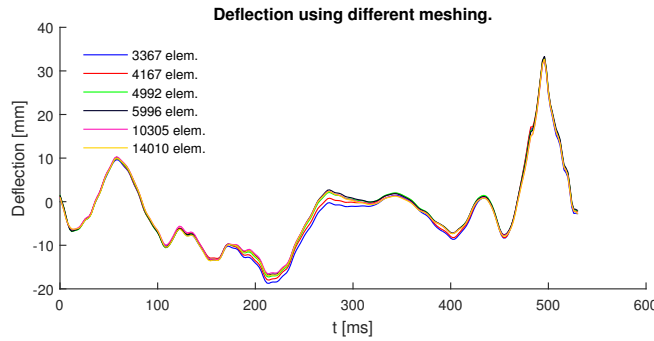


Figure 4.4: Top deflection for different refinements of the mesh, where finest has the most elements.

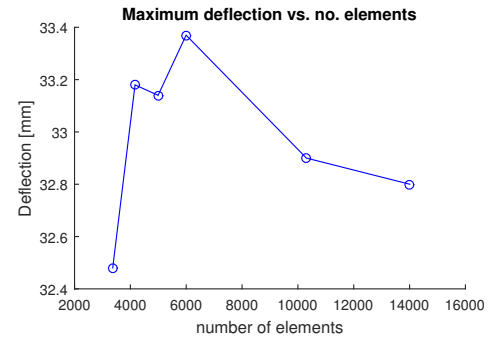


Figure 4.5: Maximum top deflection versus the number of elements.

4.4 Frequency Response and Eigenfrequencies

In Figures 4.6 to 4.9, the four eigenmodes with the lowest eigenfrequencies are illustrated where the mode shapes were the same for all racket models. The shapes indicates what type of behaviour the vibration will have when the racket is excited by acting forces. Modes one, two and four are different bending modes acting in the directions of the swing. The first and fourth mode are both acting in the forward/backwards deflection while the second mode acts in the side deflecting direction. The third mode is a twisting mode acting around the rackets longitudinal axis which also shears the head.



Figure 4.6: 1st eigenmode

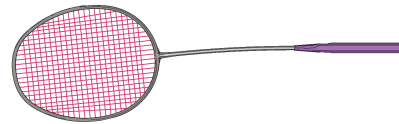


Figure 4.7: 2nd eigenmode

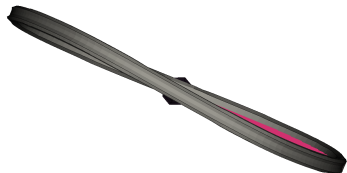


Figure 4.8: 3rd eigenmode



Figure 4.9: 4th eigenmode

The calculation extracted the first seven eigenfrequencies for each racket model. Since the simulation uses a clamped bottom on the handle there are no rigid body modes detected. In Table 4.2 the frequency values are presented for the seven eigenmodes. The four lower eigenmodes are all within the interval of 16 – 60 Hz.

Regardless of the alternations on the racket the frequency does not change significantly with an exception for the Prince racket which has an considerable lower first eigenfrequency. Further, it is clear that the frequency span of each eigenmode follows the trend where the frequency increases with a lower mass, a lower stiffness or a center of gravity closer to the handle.

The damping for the racket motion simulations is defined with the eigenfrequencies as a reference and needs to be the same for all models. The lowest and highest values from Table 4.2 set the boundaries for the damping.

	Mode 1	Mode 2	Mode 3	Mode 4	Mode 5	Mode 6	Mode 7
Original	21.8 Hz	26.1 Hz	51.9 Hz	53.3 Hz	110.7 Hz	192.1 Hz	272.3 Hz
Stiff shaft	19.7 Hz	24.9 Hz	51.9 Hz	58.4 Hz	128.1 Hz	192.1 Hz	294.4 Hz
Weak shaft	23.9 Hz	28.0 Hz	43.2 Hz	52.0 Hz	83.3 Hz	192.1 Hz	235.8 Hz
Stiff head	21.0 Hz	24.5 Hz	49.2 Hz	60.5 Hz	113.0 Hz	213.6 Hz	282.6 Hz
Weak head	23.1 Hz	29.8 Hz	37.7 Hz	56.9 Hz	106.6 Hz	152.7 Hz	252.8 Hz
High COG	21.0 Hz	24.5 Hz	49.2 Hz	60.5 Hz	113.0 Hz	213.6 Hz	282.7 Hz
Low COG	23.8 Hz	27.9 Hz	54.0 Hz	58.8 Hz	118.4 Hz	211.0 Hz	280.8 Hz
High mass	20.8 Hz	25.2 Hz	50.4 Hz	50.7 Hz	105.6 Hz	183.3 Hz	259.7 Hz
Low mass	24.2 Hz	28.3 Hz	54.4 Hz	60.2 Hz	121.6 Hz	213.8 Hz	293.3 Hz
Prince	4.5 Hz	27.5 Hz	38.0 Hz	59.8 Hz	112.0 Hz	210.7 Hz	251.9 Hz
Oval	21.1 Hz	25.4 Hz	51.2 Hz	53.5 Hz	112.0 Hz	245.4 Hz	267.0 Hz

Table 4.2: The eigenfrequencies for each mode of the models.

4.5 Clear - Racket Behaviour and Parameter Influence

The clear stroke uses relatively high force with the aim to send the shuttle with a high trajectory to the back of the opponents court. It is less powerful than the smash stroke and also has a lesser racket head speed at impact. This is shown in the following result, where the movement and deflection of the racket is presented together with the resulting shuttle velocity.

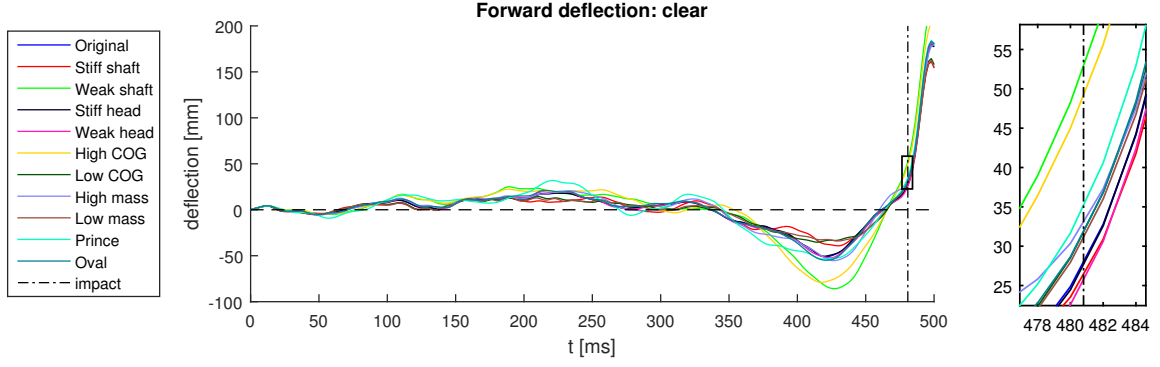
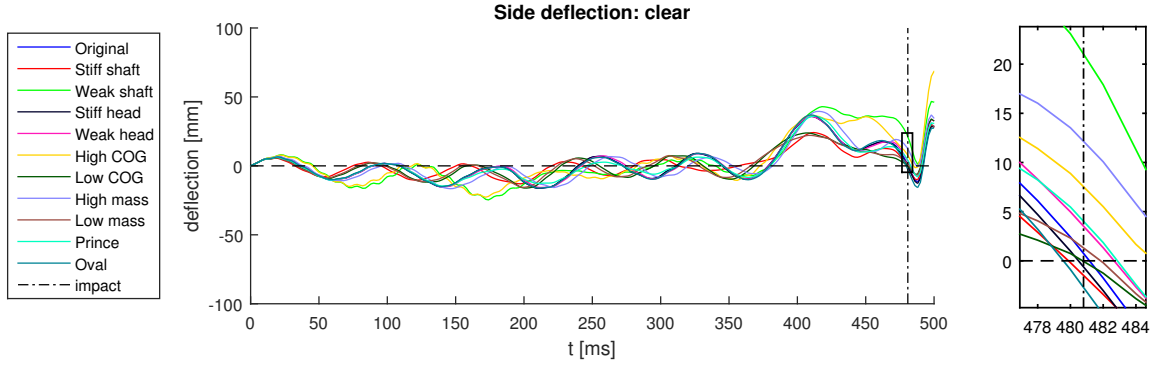
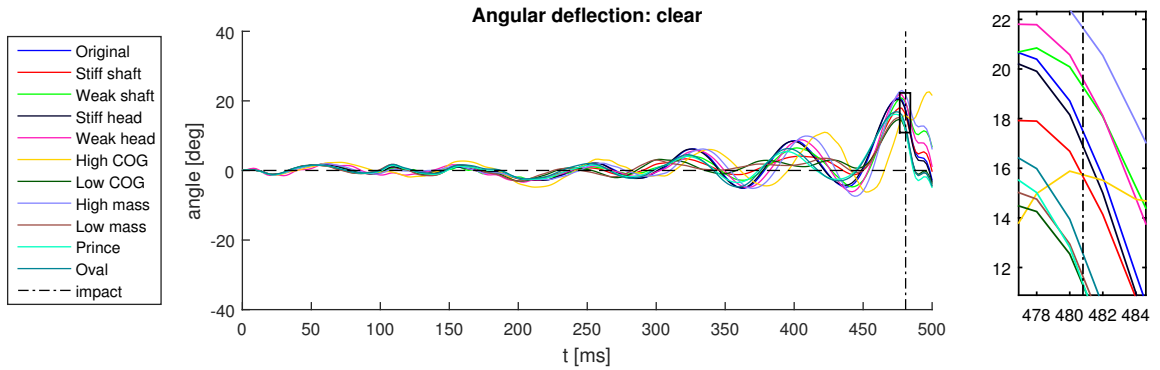
4.5.1 Deflection of Racket During Swing and Hit

In Figures 4.10 to 4.12, the elastic response in terms of deflections for bending and torsion, using the rigid models as reference, are illustrated over time for all evaluated racket models. Consequently, the deformation shown are purely the deflection and not the total movement of the racket. In all three figures there are two dotted black lines, the vertical corresponds to the time when the racket hits the ball from the motion capture data while the horizontal line indicate where zero deflection occurs. To further enhance the possibility to analyse the data the deflection behaviour close to impact are zoomed in and illustrated to the right in each picture.

The forward deflection over time is illustrated in Figure 4.10. During the first 400 ms the racket does not deflect significantly, but as the racket accelerates in the swing the bending increases. First it bends backwards and about 20 ms before impact it is neutral but with an velocity forward resulting in a deflection towards the shuttle. Consequently the rackets hits the shuttle while being deflected forward, which is true for all racket. The different rackets have similar deflections with higher center of gravity and lower shaft stiffness as exceptions.

Regarding the side deflection the behaviour is slightly different, as shown in Figure 4.11. From the start of the swing and to the point where the racket accelerates rapidly, there is a significant oscillation in the side deflection data. As the racket accelerates rapidly, roughly 350 ms into the swing, the side deflection grows to its highest pre-impact value. Most racket models do however return to a side deflection value of less than 5 mm at impact.

Similar to the side deflections, the angular deflection, illustrated in Figure 4.12, has the same type of oscillation behaviour with an sequentially increasing amplitude. The plot illustrates how the oscillations is similar throughout the swing while the amplitude increases during the last part of the sequence. Unlike the side and forward deflection the angular deflection is distributed with a lager spread within the interval of 11-22 degrees.

Figure 4.10: *Forward deflection for clear swing.*Figure 4.11: *Side deflection for clear swing.*Figure 4.12: *Angular deflection for clear swing.*

To further clarify the deflection behaviour, the values for the original racket are compared with the alternated racket models. In Table 4.3 the values for the original racket are stated at impact time. The difference is stated in percent of the value for the original. Thus if the value becomes 0% it is undeformed while 100% means that the deflection is equivalent with the original racket. Both side deflection and angular deflection indicates a trend that lower to higher values of stiffness, mass, etc. follows a roughly linear path, using original as the middle point, with the exception for the centre of gravity for angular deflection. Regarding the forward deflection the values do not indicate that type of behaviour. As the impact time is different for different rackets the maximum deflections for the different rackets are also presented in the same table and here the trend is much clearer for the forward deflection.

4.5.2 Racket Velocity at Impact

The velocities during the clear swing are shown in Figure 4.13 where the racket models during the first 100 ms are only affected by a small acceleration. Around 400 ms the acceleration increase rapidly which corresponds

	Forward deflection	Side deflection	Angular deflection	Max. forw. deflection	Max. side deflection	Max. angular deflection
Original	24.9 mm	2.42 mm	18.7 deg	180.64 mm	46.44 mm	20.87 deg
Stiff shaft	95 %	8 %	89 %	81 %	62 %	77 %
Weak shaft	194 %	954 %	107 %	144 %	124 %	88 %
Stiff head	98 %	41 %	97 %	99 %	100 %	98 %
Weak head	91 %	206 %	110 %	102 %	101 %	102 %
High COG	181 %	367 %	85 %	130 %	130 %	40 %
Low COG	115 %	31 %	67 %	84 %	76 %	51 %
High mass	122 %	559 %	120 %	105 %	101 %	105 %
Low mass	112 %	95 %	69 %	82 %	68 %	51 %
Prince	127 %	226 %	69 %	108 %	97 %	63 %
Oval	115 %	37 %	75 %	102 %	101 %	71 %

Table 4.3: The deflection of the racket at impact.

to the time when the deflection started to increase. The curve clearly shows the presence of vibrations which are less significant during the rapid part of the swing. Further the behaviour for all racket are similar and the predicted shuttle impact timing, indicated by the dotted black line, are close to racket speed maximum. By comparing the rigid body behaviour shown in Figure 4.14 to the deformable racket models in Figure 4.13 the velocity profiles up to just before the impact are nearly identical, whereby implying that the velocity is governed by the rigid body motion in the clear swing. The deformable racket models do however gain additional speed from the forward deflection of the shaft, as most of these do hit at their peak speeds while the rigid model's velocity decreases just before the time of impact.

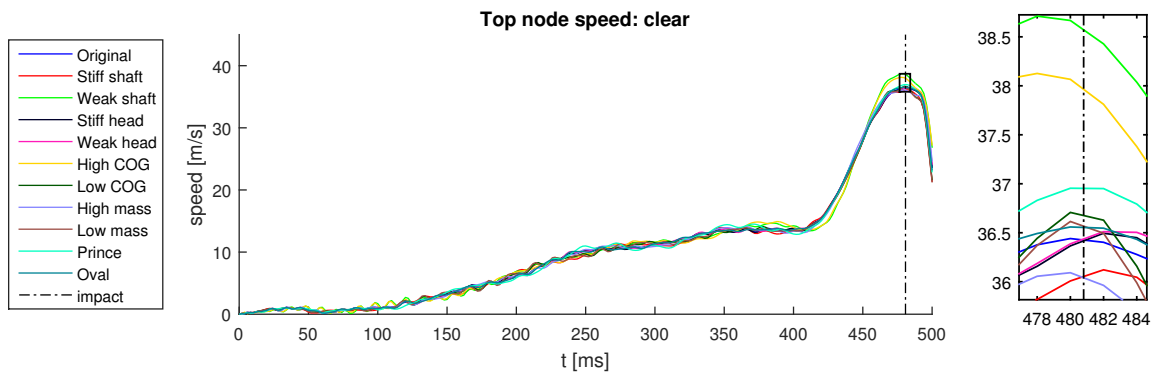


Figure 4.13: The velocities for the head tip over the time span for deformable rackets.

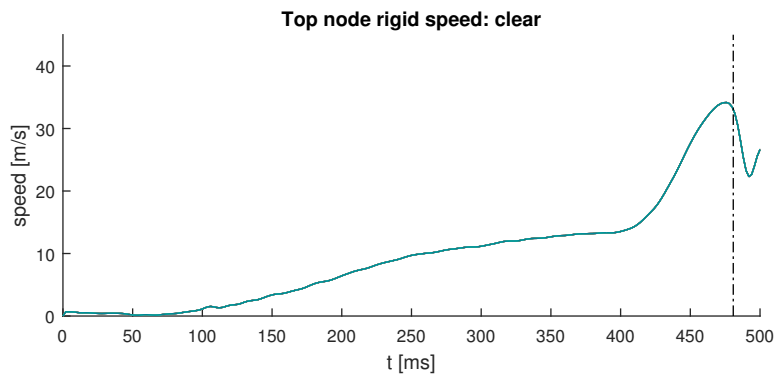


Figure 4.14: The velocities for the head tip over the time span for rigid body racket.

In Table 4.4, the two rightmost column show the total tip velocity at impact and the maximum total tip

velocity for each racket. Which shows that most racket models impact at their maximum velocity. Columns 1-4 present the velocity contribution from the deflection of the racket. One observation is that the racket with a centre of gravity closer to the head and the racket with a weaker shaft have a significant higher racket velocity at impact. The rest of the rackets have a fairly similar total velocity with a difference of ± 1 %. Although evaluation of the contribution from the deflection reveals that high mass racket and stiff racket have significantly less deflection velocity whereas the Prince racket have a higher contribution from the deflection. This does not affect the total velocity in a significant way due to the fact that the percentage might be high but the absolute value for the increase or decrease increment is low as it refers to the original value of 3.87 m/s.

	Forward defl. velocity	Side defl. velocity	Angular defl. velocity	Total defl velocity	Total velocity	Max. total velocity
Original	2.79 m/s	1.85 m/s	0.84 deg/s	2.98 m/s	36.4 m/s	36.4 m/s
Stiff shaft	86 %	83 %	73 %	85 %	99 %	99 %
Weak shaft	166 %	101 %	45 %	175 %	106 %	106 %
Stiff head	99 %	100 %	105 %	97 %	100 %	100 %
Weak head	96 %	90 %	73 %	98 %	100 %	100 %
High COG	153 %	69 %	54 %	154 %	104 %	105 %
Low COG	111 %	37 %	101 %	109 %	101 %	101 %
High mass	81 %	68 %	37 %	88 %	99 %	99 %
Low mass	106 %	48 %	108 %	106 %	100 %	100 %
Prince	116 %	75 %	131 %	117 %	101 %	101 %
Oval	105 %	111 %	121 %	104 %	100 %	100 %

Table 4.4: The deflection and total velocity at impact.

4.5.3 Momentum During Stroke

Each racket requires different amounts of momentum to complete the full stroke sequence, which is illustrated in Figure 4.15. The initial phase includes significantly much vibrations also observed in the deflection and velocity data. The major part of the parameters have low influence to the required momentum. However, difference in mass and centre of gravity influence the required momentum significantly. Additionally, close to the impact during the high speed section of the clear sequence the weaker shaft requires some extra momentum.

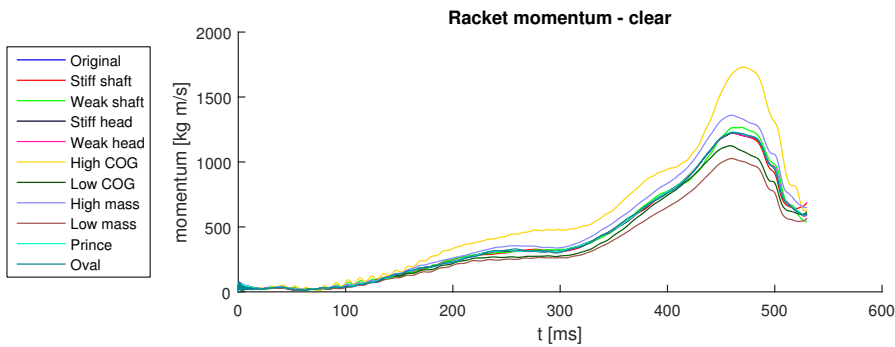


Figure 4.15: The momentum for clear swing.

4.5.4 Contact Time and Duration

For each swing-racket combination the resulting contact information for the strings and ball interaction are saved. This information is gathered at a resolution of 100 times per millisecond giving the precision shown in Figure 4.16. It can be seen that all balls aligned with the shaft axis (balls 1, 2, 4, 6 and 7) have roughly the same contact interval. The balls positioned on the sides of the head have shifted impact times. This is shown in Table A.4 in Appendix A to be true for all rackets. The balls are however positioned so that all would have almost the exact same time of initial contact, if the racket was rigid.

In Table 4.5 the average times of contact are presented and all but three rackets are found within the interval of -0.12 ms to +0.06 ms from the original value. The three rackets, which all have an impact at a later state than the original, are situated within the interval of -0.79 ms to -0.27 ms.

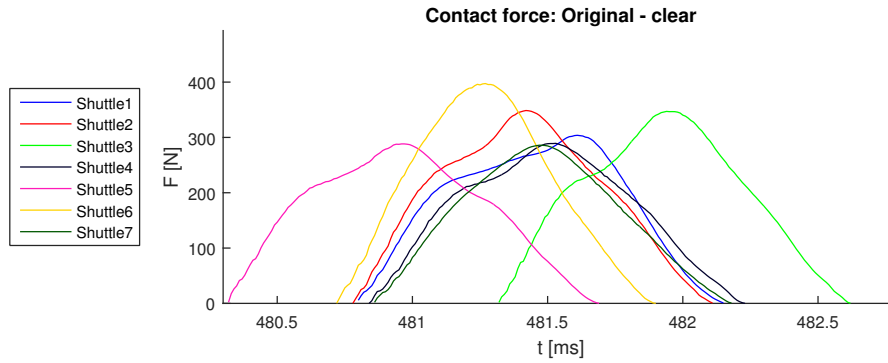


Figure 4.16: Illustration of the contact time and contact reaction force for original racket.

	Average initial contact time	Standard deviation	Shuttle 1 initial contact time
Original	480.81 ms	0.29 ms	480.8 ms
Stiff shaft	+0.06 ms	-0.03 ms	+0.06 ms
Weak shaft	-0.79 ms	+0.05 ms	-0.8 ms
Stiff head	+0 ms	-0.01 ms	+0 ms
Weak head	+0 ms	+0.06 ms	+0 ms
High COG	-0.49 ms	-0.03 ms	-0.49 ms
Low COG	-0.04 ms	-0.1 ms	-0.04 ms
High mass	-0.27 ms	+0.11 ms	-0.27 ms
Low mass	-0.04 ms	-0.09 ms	-0.04 ms
Prince	-0.12 ms	-0.1 ms	-0.12 ms
Oval	+0 ms	+0 ms	+0 ms

Table 4.5: The time difference when the shuttle first makes contact with the racket in the clear swing.

Table 4.6 represents the complete contact time for each racket and type of shuttle. The average refers to an expected average contact time if the different shuttle hits would occur equally amounts of times. Regarding the standard deviation, a percentage lower than 100% means that the distribution is less than the original racket and opposite for higher values than 100%. Note that an increase of the average value will increase the value of the standard deviation. Hence, the spread could be the same if measuring in proportion to the average value. However, an increased average contact time is not directly correlated to an increase of the standard deviation for all racket models.

	Average contact length	Standard deviation	Shuttle 1 contact length
Original	1.32 ms	0.069 ms	1.35 ms
Stiff shaft	99 %	107 %	99 %
Weak shaft	99 %	113 %	102 %
Stiff head	99 %	107 %	101 %
Weak head	102 %	106 %	101 %
High COG	99 %	99 %	99 %
Low COG	97 %	113 %	96 %
High mass	102 %	104 %	104 %
Low mass	97 %	107 %	97 %
Prince	100 %	129 %	99 %
Oval	100 %	100 %	100 %

Table 4.6: The difference in length of contact for the different impacts in the clear swing, compared to original racket. In milliseconds.

4.5.5 Shuttle Velocity and Direction

The post-impact velocity of the shuttle is shown in Table 4.7 for the clear swing. These are all close to the value from the speed measured in the motion capture study, which was 49.5 m/s. The highest shuttle speed was measured in the high COG simulation at 50.2 m/s and the lowest in the high mass simulation at 36.4 m/s. All speeds are however in the range of ± 10 % from the original model. For all rackets, there is a clear trend that with greater speed average comes higher variation in speed, except for the weak shaft model.

The coefficient of restitution, COR, is a measurement which correlates the gain in shuttle velocity to the drop in racket velocity due to the impact, see Section 2.1.3. A high value means that the racket has transferred more of its kinetic energy to the shuttle. In Table 4.17, these values are shown where the high COG model has the greatest COR result and high mass the smallest, correlating well with the shuttle speed results.

In Table 4.18 the angle of trajectory is shown, measured as described in Section 3.9.3. It is clear that the Prince model has the lowest average angular offset as well as the least variation, while high COG has the greatest.

	Average shuttle speed	Standard deviation	Shuttle 1 speed
Original	45.1 m/s	3.64 m/s	46.4 m/s
Stiff shaft	101 %	103 %	101 %
Weak shaft	98 %	107 %	98 %
Stiff head	101 %	106 %	101 %
Weak head	97 %	96 %	97 %
High COG	109 %	109 %	108 %
Low COG	102 %	104 %	102 %
High mass	93 %	98 %	93 %
Low mass	101 %	103 %	101 %
Prince	106 %	107 %	106 %
Oval	100 %	100 %	100 %

Table 4.7: The difference in speed of the ball post impact compared to the original racket in the clear swing. In meters per second.

	Average COR	Standard deviation	Shuttle 1 COR
Original	0.62	0.136	0.69
Stiff shaft	105 %	103 %	107 %
Weak shaft	83 %	87 %	91 %
Stiff head	102 %	105 %	101 %
Weak head	92 %	93 %	96 %
High COG	113 %	113 %	106 %
Low COG	108 %	104 %	109 %
High mass	83 %	112 %	83 %
Low mass	107 %	104 %	106 %
Prince	114 %	104 %	110 %
Oval	100 %	100 %	100 %

Figure 4.17: Coefficient of restitution.

	Average shuttle trajectory offset	Standard deviation
Original	0.9 deg	0.63 deg
Stiff shaft	80 %	94 %
Weak shaft	99 %	83 %
Stiff head	88 %	113 %
Weak head	103 %	91 %
High COG	95 %	64 %
Low COG	80 %	57 %
High mass	74 %	66 %
Low mass	69 %	44 %
Prince	32 %	24 %
Oval	100 %	100 %

Figure 4.18: The offset in shuttle trajectory post impact, measured from ball 1 trajectory in the horizontal plane, in the clear swing.

4.5.6 Repositioned Ball

By reposition the shuttles denoted as number 1 the shuttle velocities for different time of impacts is obtained. For the clear stroke these velocities are presented in Table 4.8. For the clear stroke the original time of impact is counted as the middle stroke due to the velocity profile illustrated in Figure 4.13, while the two other strokes are 2 ms earlier and later respectively. In Figure 4.19 the time of impact is illustrated for the different simulations. This two other impact times gives a lower shuttle velocity for all but the high COG racket and the Oval racket.

The racket with a centre of gravity closer to the head have almost unaffected velocity regardless of the three impacts. For the Oval racket the middle impact gives the highest velocity. It is also clear that some parameters make the racket more or less affected by the impact time which is illustrated in the three columns defining the difference from the original racket. For instance, the stiffness of the head gives the same behaviour as the original racket with an decreasing velocity whereas a stiffer shaft have a slightly less distribution of shuttle velocities for different impacts.

	Shuttle vel. early impact	Shuttle vel. orig. impact	Shuttle vel. late impact	Shuttle vel. early impact	Shuttle vel. orig. impact	Shuttle vel. late impact
Original	44.1 m/s	46.4 m/s	45.5 m/s	44.1 m/s	46.4 m/s	45.5 m/s
Stiff shaft	103 %	101 %	102 %	45.2 m/s	46.8 m/s	46.2 m/s
Weak shaft	101 %	98 %	99 %	44.5 m/s	45.7 m/s	45 m/s
Stiff head	101 %	101 %	101 %	44.5 m/s	46.7 m/s	45.8 m/s
Weak head	97 %	97 %	97 %	42.6 m/s	45.2 m/s	44.2 m/s
High COG	114 %	108 %	111 %	50.4 m/s	50.2 m/s	50.3 m/s
Low COG	106 %	102 %	104 %	46.5 m/s	47.5 m/s	47.1 m/s
High mass	95 %	93 %	94 %	41.7 m/s	43.3 m/s	42.6 m/s
Low mass	104 %	101 %	102 %	45.7 m/s	46.9 m/s	46.5 m/s
Prince	109 %	106 %	107 %	47.9 m/s	49.2 m/s	48.7 m/s
Oval	106 %	100 %	105 %	46.6 m/s	46.4 m/s	48 m/s

Table 4.8: The difference when the shuttle has been moved for the clear swing.

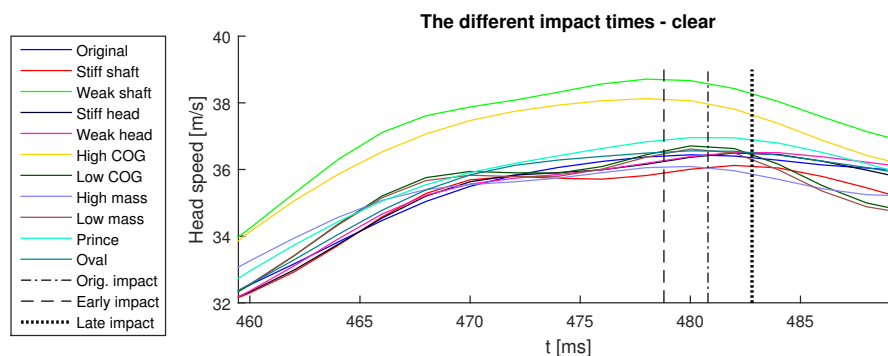


Figure 4.19: The impact times of the repositioned shuttles. The early impact is -2 ms and the late is $+2$ ms in relation to the original impact.

4.6 Smash - Racket Behaviour and Parameter Influence

The smash stroke uses high force with the aim to win the point by giving the shuttle a high velocity and a steep trajectory towards the other opponents court. It is far more powerful than the clear stroke and also has a the highest racket head speed at impact. This is shown in the following result, where the movement and deflection of the racket is presented together with the resulting shuttle velocity.

4.6.1 Deflection

The smash was simulated during period of 602 ms compared with 530 ms for the clear stroke. The deformation for forward, side and angular deflection is illustrated in Figures 4.20-4.22. One common behaviour for all deflections is the presence of vibration as all graphs show a significant oscillation behaviour.

For the forward deflection the oscillation is present during the total smash sequence. The amplitudes are low for all rackets during the first 250 ms. Subsequently, the deflection increases and around 500 ms there is a large backwards deflection which almost reaches the normal position before the impact of the shuttle. The zoomed area reveals that the rackets are backwards deflected in an interval of 15 – 42 mm at the time the

motion capture data reach impact.

In Figure 4.21 a similar behaviour is illustrated for the side deflection with a significant oscillation. The graph shows that vibration in the side deflection is more significant during the period prior 500 ms. At that time the rackets rapidly deflect to one side but some manage to flex back and pass the normal position before the impact of the shuttle. The zoomed area shows that during the motion capture impact time most of the racket have an deflection towards the opposite side than during the first acceleration phase. Three racket are still deflected in the first direction while the high mass racket is undeformed.

While the side deflections varies around zero at impact time, the angular deflections are all above zero at the motion capture impact. Figure 4.22 illustrates the angular deflection over time and as the black dotted line indicates there is a relative large deflection at the time when the motion capture data hits the shuttle and thus similar deflection occurs during the simulated impact. The vibration for the angular deflection indicates large oscillations for the complete smash sequence. The magnified picture shows that the span for the angle is between 15 – 22 degrees at impact.

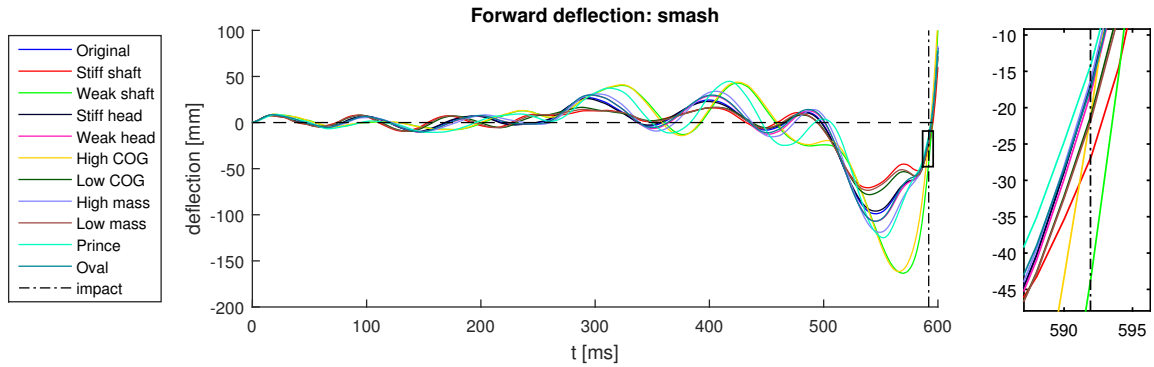


Figure 4.20: *Forward deflection for smash swing.*

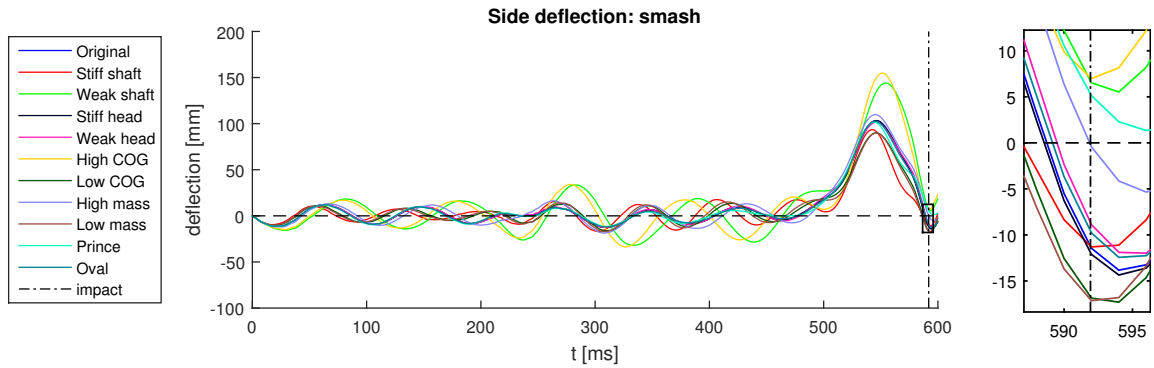


Figure 4.21: *Side deflection for smash swing.*

Table 4.9 shows the deflection of the original racket at the simulated time of impact for the centre shuttle, also referred as shuttle 1. These are compared with the same values for the alternated rackets and presented as a percentage of the original racket's values. The angular deflection is the least affected deflection parameter for the racket with a span of 83 – 115%. The forward deflection lies within the span of 66 – 150% where the high COG racket has the most deflection. Regarding side deflection the span is the biggest with a spread between 43 – 312% although the forward deflection is of a much larger magnitude meaning that the spread may be higher for the side deflection but not the absolute values.

4.6.2 Racket Velocity at Impact

The top node velocity for each racket during the smash is illustrated in Figure 4.23. During the first 270 ms there are mostly small accelerations and noise from the motion capture data. The next section between 270-520 ms there are steady and roughly constant accelerations followed by a small dip before a rapid acceleration occurs during the last section until impact. In the magnified area, the different lines indicate that the velocity

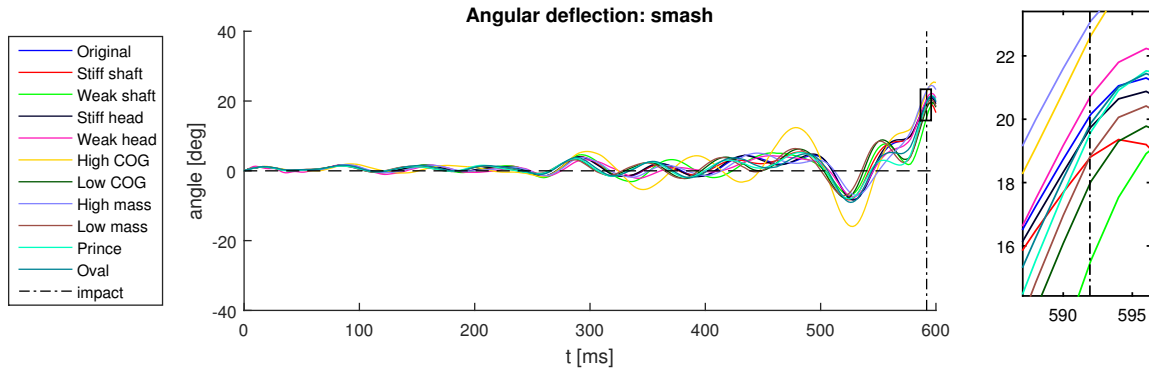


Figure 4.22: Angular deflection for smash swing.

	Forward deflection	Side deflection	Angular deflection	Max. forw. deflection	Max. side deflection	Max. angular deflection
Original	28.8 mm	5.5 mm	18.7 deg	81.14 mm	103.4 mm	21.3 deg
Stiff shaft	92 %	205 %	100 %	72 %	76 %	95 %
Weak shaft	149 %	119 %	83 %	135 %	129 %	76 %
Stiff head	100 %	114 %	98 %	98 %	100 %	100 %
Weak head	104 %	43 %	102 %	106 %	100 %	95 %
High COG	150 %	180 %	111 %	133 %	133 %	122 %
Low COG	72 %	307 %	96 %	80 %	85 %	80 %
High mass	97 %	116 %	115 %	114 %	109 %	104 %
Low mass	74 %	312 %	101 %	77 %	83 %	77 %
Prince	86 %	192 %	94 %	109 %	96 %	82 %
Oval	99 %	67 %	97 %	105 %	99 %	92 %

Table 4.9: The deflection of the racket at impact.

is higher at a time after the shuttle hit from the motion capture data. This is true for all rackets. Although, by evaluating Figure 4.24 the rigid body velocity shows that the maximum top node velocity is at the moment of impact. Similar as for the clear stroke, the badminton racket experience a rapid deceleration immediately after the impact with the shuttle.

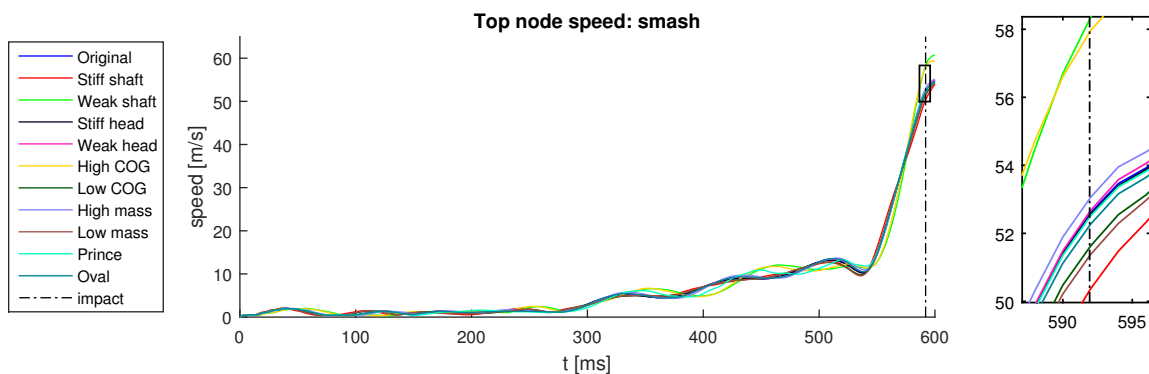


Figure 4.23: The velocities for the head tip over the time span for deformable rackets.

The top node velocity for each deformable racket can be reviewed in Table 4.10. The velocity is taken at the simulated time of impact. Thus, the real time differs depending on when the racket actually hits the shuttle. The column to the right contains the total velocities where all but two rackets falls within the interval of 98 – 101% of the original rackets velocity. The racket with weaker shaft and a centre of gravity closer to the head have an increased velocity of 111% and 108% respectively. The other columns include the different contributions from the three different measured deformations. The stiff shaft have an significantly

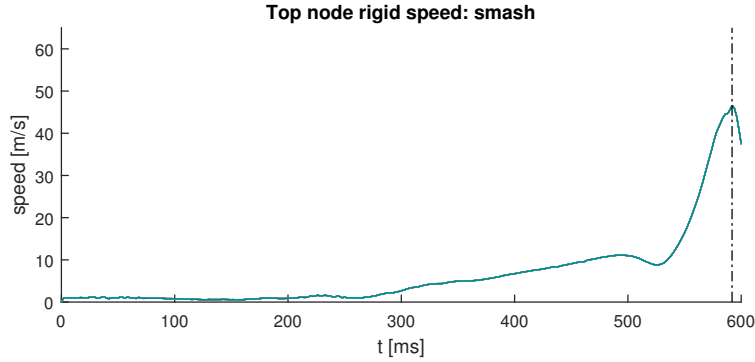


Figure 4.24: The velocities for the head tip over the time span for rigid body racket.

lower deformation velocity while the two fastest racket have an significantly higher deformable velocity. The rest of the rackets lie within the interval of 80 – 107%. Further, the result indicates different trends for the evaluated parameters. For instance the shaft stiffness seems to have a roughly linear correlation between higher stiffness and lower total velocity.

	Forward defl. velocity	Side defl. velocity	Angular defl. velocity	Max. forward defl. velocity	Max.side defl. velocity	Max. angular defl. velocity
Original	5.71 m/s	4.37 m/s	0.74 deg/s	5.98 m/s	51.4 m/s	54.8 m/s
Stiff shaft	77 %	34 %	76 %	63 %	98 %	98 %
Weak shaft	209 %	65 %	168 %	196 %	113 %	111 %
Stiff head	100 %	99 %	100 %	99 %	100 %	100 %
Weak head	97 %	105 %	115 %	101 %	100 %	100 %
High COG	197 %	76 %	119 %	186 %	110 %	108 %
Low COG	99 %	49 %	132 %	84 %	100 %	99 %
High mass	99 %	103 %	109 %	107 %	101 %	101 %
Low mass	96 %	39 %	130 %	80 %	100 %	99 %
Prince	90 %	84 %	143 %	99 %	100 %	99 %
Oval	92 %	100 %	127 %	95 %	99 %	100 %

Table 4.10: The deflection and total velocity at impact.

4.6.3 Momentum During Stroke

Similar to the clear stroke, the results for the smash stroke give the same behaviour for the required momentum, see Figure 4.25. Centre of gravity and the mass of the racket have a significant influence on the momentum. During the last section of the smash sequence, a significant influence from the shaft stiffness is observed.

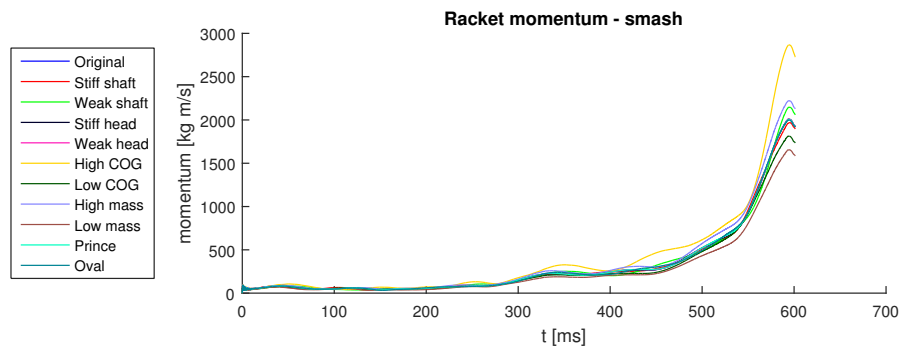


Figure 4.25: The momentum for smash swing.

4.6.4 Contact Time and Duration

In Table 4.11 the time of initial contact is stated for the centred shuttle and the average if all the different shuttle hits would occur equal amounts of time. For the smash stroke, the average contact is at 591.94 ms for the original racket and the rest of the rackets lie with an interval of -0.23 ms to +0.31 ms from that value. The standard deviation has a value between 0.19-0.35 ms which indicates that the contact time deviates with roughly the same magnitude for different rackets as for different shuttle impacts. Looking at the different material parameters the mass and COG has a clear trend while the shaft stiffness has an increase initial impact time for both lower and higher stiffness.

	Average initial contact time	Standard deviation	Shuttle 1 initial contact time
Original	591.94 ms	0.28 ms	591.93 ms
Stiff shaft	+0.14 ms	-0.01 ms	+0.14 ms
Weak shaft	+0.31 ms	-0.09 ms	+0.31 ms
Stiff head	+0.01 ms	-0.01 ms	+0.01 ms
Weak head	-0.02 ms	+0.03 ms	-0.02 ms
High COG	-0.1 ms	+0.02 ms	-0.09 ms
Low COG	+0.11 ms	-0.03 ms	+0.1 ms
High mass	-0.14 ms	+0.07 ms	-0.14 ms
Low mass	+0.13 ms	-0.02 ms	+0.12 ms
Prince	-0.23 ms	-0.01 ms	-0.23 ms
Oval	-0.02 ms	+0 ms	-0.02 ms

Table 4.11: The time difference when the shuttle first makes contact with the racket in the smash swing.

To further evaluate the time spectra of the impact, the contact time is presented in Table 4.12. The impact time is low regardless which parameter that is simulated, although there are small differences giving an interval of 1.16-1.33 ms in average contact time if all the different ball impacts would occur with the same frequency. For some parameters, the trend how an increase/decrease affect the contact is clear. Other parameters have a more diffuse influence on the contact behaviour.

	Average contact length	Standard deviation	Shuttle 1 contact length
Original	1.2 ms	0.102 ms	1.25 ms
Stiff shaft	100 %	114 %	101 %
Weak shaft	103 %	61 %	104 %
Stiff head	100 %	103 %	99 %
Weak head	102 %	103 %	102 %
High COG	107 %	72 %	101 %
Low COG	98 %	106 %	100 %
High mass	105 %	97 %	102 %
Low mass	97 %	101 %	98 %
Prince	104 %	99 %	102 %
Oval	99 %	105 %	99 %

Table 4.12: The difference in length of contact for the different impacts in the smash swing, compared to original racket. In milliseconds.

4.6.5 Shuttle Velocity and Direction

Shuttle speeds for all the smash simulations are shown in Table 4.13. The average speed are the same as in the original model for the majority of the simulations, but the shuttle velocity for the weak shaft and high COG results are significantly higher. These two also have the highest variation in shuttle speeds where the increase in standard deviation of the speed is not proportional to the rise in average speed. The lowest average speed was observed in the high mass model which too has a disproportionally large variation in its shuttle speeds.

In the analysis of the clear swing the COR values correlated well with the shuttle speeds. This is not as obvious for the smash swing, shown in Table 4.26. Especially the high COG model, which had the second highest average speed, has a low COR value. The highest COR value is found in the high shaft stiffness model meaning that it is the model which transfers the highest percent of its kinetic energy to the ball, of all the models. The model which transfers the least of its kinetic energy is the high mass model.

The post-impact trajectory of the shuttle is shown in Table 4.27. There is a clear trend that the stiff models and the low COG model have a significantly lower average angular offset, where the stiff head model has the lowest value. The opposite effect can be seen for their counterpart models where high COG has the biggest average angular offset. Both the high and low mass models have a worse average than the original model, although both also have a lower standard deviation. The oval racket model performs well with both a low average and a low standard deviation.

	Average shuttle speed	Standard deviation	Shuttle 1 speed
Original	57.3 m/s	4.02 m/s	59.8 m/s
Stiff shaft	101 %	101 %	101 %
Weak shaft	111 %	169 %	113 %
Stiff head	101 %	103 %	101 %
Weak head	97 %	93 %	97 %
High COG	107 %	154 %	109 %
Low COG	100 %	96 %	101 %
High mass	94 %	108 %	94 %
Low mass	99 %	94 %	99 %
Prince	100 %	115 %	99 %
Oval	100 %	104 %	100 %

Table 4.13: The difference in speed of the ball post impact compared to the original racket in the smashwing. In meters per second.

	Average COR	Standard deviation	Shuttle 1 COR
Original	0.4	0.122	0.43
Stiff shaft	121 %	106 %	135 %
Weak shaft	109 %	142 %	128 %
Stiff head	104 %	103 %	105 %
Weak head	90 %	93 %	93 %
High COG	88 %	116 %	102 %
Low COG	114 %	105 %	133 %
High mass	72 %	85 %	84 %
Low mass	110 %	103 %	128 %
Prince	100 %	93 %	112 %
Oval	102 %	103 %	105 %

Figure 4.26: *Coefficient of restitution.*

	Average shuttle trajectory offset	Standard deviation
Original	0.655 deg	0.825 deg
Stiff shaft	87 %	91 %
Weak shaft	240 %	183 %
Stiff head	69 %	50 %
Weak head	157 %	93 %
High COG	473 %	763 %
Low COG	97 %	70 %
High mass	114 %	98 %
Low mass	118 %	76 %
Prince	120 %	95 %
Oval	74 %	59 %

Figure 4.27: *The offset in shuttle trajectory post impact, measured from ball 1 trajectory in the horizontal plane, in the smash swing.*

4.6.6 Repositioned Ball

Just as for the clear stroke different times of impact is evaluated by reposition the shuttle for the smash stroke. The obtained shuttle velocities from these simulations are presented in Table 4.14. For the smash stroke the original time of impact is defined as the earliest stroke due to the velocity profile illustrated in Figure 4.23, while the two other strokes are simulated 2 ms and 4 ms later respectively. In Figure 4.28 the time of impact is illustrated for the different simulations. The trend is not as obvious as for the clear stroke, for the original racket the lowest shuttle speed is for the middle impact. Although for most rackets the trend is that the middle impact gives the highest velocity with the weak shaft giving the absolute highest shuttle velocity of 72 m/s.

The columns illustrating the difference between the original racket and the rackets with alternated parameters give no certain trend although it is clear that some parameters are affected more than others for different initial impact times.

	Shuttle vel. orig. impact	Shuttle vel. late impact	Shuttle vel. later impact	Shuttle vel. orig. impact	Shuttle vel. late impact	Shuttle vel. later impact
Original	59.8 m/s	57.5 m/s	60.9 m/s	59.8 m/s	57.5 m/s	60.9 m/s
Stiff shaft	101 %	99 %	107 %	60.6 m/s	57.1 m/s	65.3 m/s
Weak shaft	113 %	125 %	101 %	67.8 m/s	72 m/s	61.5 m/s
Stiff head	101 %	100 %	100 %	60.5 m/s	57.5 m/s	60.9 m/s
Weak head	97 %	100 %	98 %	58.2 m/s	57.4 m/s	59.9 m/s
High COG	109 %	111 %	94 %	64.9 m/s	63.8 m/s	57.2 m/s
Low COG	101 %	108 %	99 %	60.6 m/s	62.4 m/s	60.1 m/s
High mass	94 %	100 %	82 %	56.2 m/s	57.8 m/s	49.8 m/s
Low mass	100 %	106 %	97 %	59.5 m/s	61.3 m/s	59.2 m/s
Prince	99 %	105 %	89 %	59.4 m/s	60.6 m/s	54.4 m/s
Oval	100 %	107 %	100 %	59.9 m/s	61.5 m/s	60.6 m/s

Table 4.14: The difference when the shuttle has been moved for the smash swing.

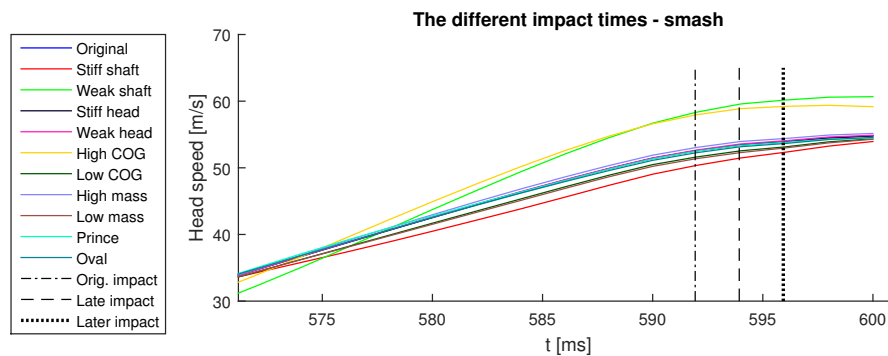
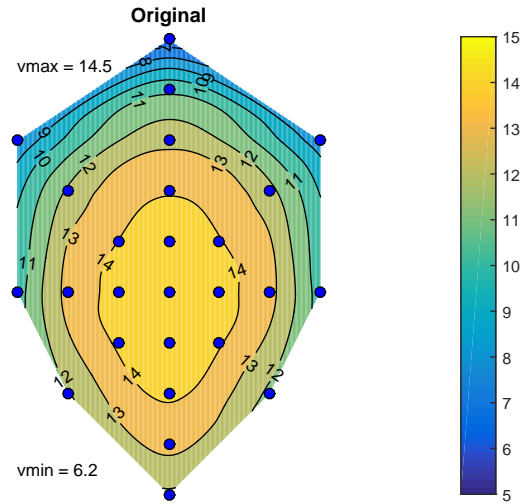


Figure 4.28: The impact times of the repositioned shuttles. The time late impact is +2 ms and the later +4 ms in relation to the original impact.

4.7 Sweet Spot Analysis for Clamped Racket

In Figure 4.29 the calculated sweet spot for the original racket is illustrated. The interpolated values gives a contour plot over almost the entire stringed area. There are still some of the outer sections that are not included as no shuttles were evaluated close to the edge. The more yellow area give a higher shuttle re-bound velocity while the blue areas close to the edges have lower velocities. In Appendix B, the sweet spot can be evaluated for each simulated racket.

The average shuttle velocity and the min/max value can be reviewed in Table 4.15. The standard deviation gives an indication if the gradient is high or low from the centred shuttle and out towards the edge. The average value is higher for most of the rackets apart from the low mass racket and the racket with lower center of gravity. On the other hand, the maximum velocity is a bit lower for most of these rackets, the only racket which gives an increased maximum velocity is the Prince racket.

Figure 4.29: *The sweetspot for original racket.*

	Average shuttle vel.	Standard deviation	Minimum shuttle vel.	Maximum shuttle vel.
Original	12.4 m/s	2.2 m/s	6.2 m/s	14.5 m/s
Stiff shaft	103 %	114 %	93 %	97 %
Weak shaft	104 %	116 %	92 %	97 %
Stiff head	103 %	117 %	86 %	97 %
Weak head	104 %	101 %	133 %	97 %
High COG	103 %	117 %	86 %	97 %
Low COG	96 %	113 %	112 %	93 %
High mass	107 %	111 %	102 %	100 %
Low mass	95 %	113 %	108 %	92 %
Prince	108 %	108 %	121 %	101 %
Oval	106 %	116 %	93 %	99 %

Table 4.15: Sweet spot data for the different models.

5

Discussion

In this section the result and the used method are discussed and possible explanations of the observed racket responses are presented. First the more general subjects are considered regarding racket motion, stiffness calibration and the dynamic responses from the eigenfrequency calculation. Subsequently the different parameters are discussed for the different racket responses followed by the assumptions and possible errors that could affect the results.

5.1 Racket Motion

The transfer from a real-life swing into a simulated swing required several steps which all reduce the accuracy of the final result. The motion capture system is limited by its recording frequency and resolution when tracking objects. The MATLAB code which reposition and smooth out the position data also reduces the accuracy. The subsequent application of this position data in the model to make it move as in real-life is then also subject to how well the model reproduces the properties of the real racket. The FE-model is however not based on the same rackets that were used in the motion captures, whereby it is interesting but not necessary if it fully replicates the motion as the it is the relative difference that is evaluated in the result.

From Figures 4.1 and 4.2 it is evident that the motion in the clear and smash simulations closely follow the motion capture movement. The greatest difference is seen in the smash swing, which can be attributed to the higher racket velocity. It is also possible that the racket used in the smash motion capture is stiffer than the one used in the clear motion capture, whereby the FE-model would model the clear motion better.

5.2 Calibration of FE-model

By evaluating the results in Section 4.2 the results indicate a similar bending deflection as the one obtained in the experimental test. The difference is that the bending stiffness is 34.5% lower than in the prototypes. The problem was that the geometry was not to be changed and as the Young's modulus that controls the stiffness also controlled the required time step, a stiffer racket would consequently result in a more expensive simulation regarding computational time. But accuracy is still important to obtain a trustworthy simulation. One could have used mass scaling to deal with this problem regarding time step but that will also introduce errors and uncertainties which could compromise the results. Another approach is to change the composite structure for the shaft by either define a different orientated layup or a thicker layup.

Even though the racket has a slightly less stiff material, the major parts of the results are still valid as the approach is to evaluate the relative difference between the different rackets. And as discussed in Section 5.1 the racket follows the motion capture data relative well. Additionally, to obtain the exact behaviour corresponding the given prototypes several properties are required such as the exact material data, shear stiffness and calibration for other elastic responses. Furthermore, the motion capture must be done using the prototype rackets.

Regarding the mesh convergence study, the results indicate that the total behaviour for the tip displacement is similar for the different resolutions. However, no steady state was obtained for the maximum tip displacement and further investigation was not possible due to time and computational limits. The used mesh discretisation for the model was picked to enable the large amounts of simulation to be possible to run. The convergence result illustrates that the chosen mesh is situated after the steepest part of the convergence but it also indicates that a finer mesh is required to be fully converged.

5.3 The Natural Frequency Response

An interesting observation is that regardless of the evaluated shape or racket parameters, the first four modes had an identical shape. Consequently, the racket dynamic behaviour is similar, with small differences in frequency, regardless of the alternation of the racket parameters evaluated in the project. This means that one could expect that the racket responses are similar even with change of properties. Comparing the explicit and modal analysis result shows that the three lowest eigenmodes govern the general racket behaviour for both the clear and smash which further proves that the racket dynamics is not significantly affected by differences of the key parameters within the evaluated intervals.

Note that one problem with this model is the applied motion and the boundary condition defining it. As the motion is prescribed, the bottom of the handle works as a rigid clamped section. This means that vibrations and deflection behaviours are affected by this. Regarding the vibration, there is a small introduced damping which slowly fade out the vibrations, but as no hand is modelled to absorb them they will occur under a longer period of time in the racket. Further, the clamped boundary give rise to vibrations that otherwise would not be visible in the racket. It can easily be illustrated by putting the handle of the racket on the edge of a table letting the shaft and head hanging in the air. By pressing the handle towards the table and simultaneously bend and release the head vibrations will occur for a significantly long time. This vibrations would otherwise be absorbed by the hand which is neither rigid nor still. The vibration data is still of use as the vibrations is absorbed by the player consequently supplying feedback to the player regarding shuttle impact and swing. Thus rackets with eigenfrequencies closer to the frequency of the applied motion will give the player a more significant feedback, that for some enhance the total performance.

5.4 Racket Responses for Key Parameter Variations

The major part of this thesis is to evaluate different racket parameters that could affect the racket response and consequently the racket performance. As no cross test data is available with several alternations of parameters in the same model, it is suitable to evaluate and discuss the different parameters independent of each other.

5.4.1 Centre of Gravity

From the manufacturers marketing of rackets the expectation is that a racket with a high COG should give a higher shuttle velocity while the low COG racket should require less effort to move. The last part is true physically. An object requires more force to move if the COG is further away from where the force is applied, which is illustrated by the momentum data. Comparing to the original racket, a centre of gravity closer to the head increased the needed momentum. No other key parameter had such influence as the centre of gravity, additionally putting the centre of gravity closer to the handle had not as much influence as placing it closer to the head. Thus, the dependence is not linear and an optimum regarding this is possible to find.

The velocities are studied, and it can be seen that in both the clear and smash simulations the high COG racket achieves significantly higher maximum racket speed (+5% and +8%) and is faster than the original racket at impact. This results in higher shuttle velocities for both swings. The result of the low COG racket is more convoluted, having a higher maximum speed in the clear stroke and a lower maximum speed in the smash stroke, albeit by only 1% in both cases which is a negligible difference. The post-impact speed of the shuttle is similar to that of the original model.

The trend for the shuttle speed using different COG is not fully clear as, from the marketing standpoint, the expectation was to see an incline in shuttle speed from higher COG and a decline from lower COG. It might be that the original model has a COG which, in relation to its other properties, is already so low that lowering it further does not have an effect on shuttle velocity. It is however clear that with a higher COG than that of the original model, the contribution from the deflection of the racket increases the racket speed and that the post-impact shuttle speed is higher. It should also be considered that more force is required to swing the high COG racket.

Another unclear trend is that higher COG gives a higher spread in shuttle trajectories, depending on where on the racket head the shuttle makes contact. For the clear stroke, the high COG model actually has a lower spread than the original model. This is not the case in the smash stroke where the high COG model has a much greater variation in the shuttle direction. This can be related to the angular deflection at impact, where in the clear stroke the high COG has a lower angular deflection and a lower angular deflection velocity contributing

to a more uniform trajectory of the shuttles. The opposite can be seen in the smash stroke leading to a higher spread. For the low COG model, these values are consistently low, resulting in the shuttle trajectory variation always being lower than the original model.

When the time of impact was moved for the clear simulation it can be seen that the original and low COG model peak in shuttle velocity when hit 2 ms later than in the parametric study. The high COG model has a almost constant shuttle velocity of 50.3 m/s for all hits. This consistency is not seen in the smash swing where high COG peaks at the first impact time and subsequently decreases significantly. The low COG peaks in the middle impact time, and like in the clear stroke has lesser shuttle speed variation depending on when hit.

Also, in the sweet spot analysis it is noticed that the low COG racket has a more consistent performance. It has a bigger lowest and a smaller highest rebound shuttle speed. The high COG would still be preferable for an experienced player, as it produces higher shuttle velocities for nearly all of the impact positions. This means that a player who can control where on the string bed contact is made also will have greater post impact shuttle speeds.

5.4.2 Mass

As discussed in Section 2.1.1 the badminton rackets have become significantly lighter since the first designs. It is clear that reducing the weight from a old heavy wooden racket to a light composite racket is beneficial as less force is required to move the racket which enable higher swing speeds. However, studies show that as the weight has been greatly reduced, the same trend is not valid within smaller weight decreasing increments. To demonstrate this one can try to throw a really light ball and compare it with throwing a tennis ball. None of the objects weighs considerably much but the really light object will not give enough feedback to be thrown correctly. This event was hard to validate with the simulations done in the project as regardless of weight, or any other changes of parameters, the prescribed motion was the same. However, the momentum data indicates that the required force to replicate the motion is different depending on racket weight. A higher mass require more momentum and the dependence shows a close to linear behaviour for the evaluated masses. This knowledge needs to be connected to the swing motion and swing speed by experimental work to enable conclusions regarding mass of racket and its influence on the racket motion.

By evaluating the racket speed it shows little difference in increased/decreased speed but the high mass racket have a higher deflection when including the maximum deflection. Although the result indicates that the increased mass does not increase the deformable velocities significantly but rather decreases it for the clear swing, which could indicate that even though it deflects more the mass is slower to deflect back to its normal position.

Regarding shuttle speed using this prescribed motions, there is a disadvantage for a heavier racket. The trend is clear when reviewing the COR value that a heavier racket have a lower value and opposite for a low mass racket. This could partly depend on the longer contact time for a heavier racket. Further, by evaluating the data for different initial impact time it confirms that the racket with higher mass gives a lower shuttle speed. Thus, the difference between this study and experimental studies is most likely explained by the applied motion. The data from the sweet spot analysis for the fixed racket further confirm that it is the applied motion that could affect these values in experiments as the measured sweet spot is larger with a higher maximum velocity than the low mass racket even though it stagnate as the maximum velocity is more or less the same as for the original racket. Note that the high mass have a better consistency regarding the shuttle speed as the minimum shuttle velocity is higher than for the original racket.

5.4.3 Shaft Stiffness

According to previous studies, see Section 2.1.2, a decrease in shaft stiffness should result in a positive contribution to racket head speed from the re-deflecting shaft. The results also show this, where both of the weak shaft strokes show a higher racket speed at impact than the original. The stiff shaft model shows the opposite effect where the reduced flexing of the shaft leads to a lesser head speed at impact.

The resulting post-impact shuttle speed indicates that this weaker shaft does not always have a positive effect. While it produces higher shuttle speed in the smash stroke, the opposite effect is seen in the clear stroke. This is probably be due to the racket having a greater forward deflection in the clear stroke and a greater forward deflection velocity in the smash stroke. If so, it indicates that the weak shaft is highly dependant on timing of the stroke. This effect is clearly seen when the impact time was moved for the smash swing. The weak shaft model had the greatest shuttle speed at 72 m/s when hit 2 ms later than in the parametric study,

but when impact was delayed an additional 2 ms the shuttle speed dropped to 61.5 m/s. This dependence on impact put high demands on the player regarding timing and consistency in the stroke as badminton is the fastest racket sport in the world.

The stiff shaft model performs similar to the original racket model in shuttle speed, but is more consistent in its execution. This is especially true for the post-impact trajectory of the shuttle where the spread is less than both the original and weak shaft model. The weak shaft has an equal variation of trajectory in the clear stroke, but in the smash stroke the average shuttle angle is more than double that of the original model and almost three times that of the stiff shaft.

The sweet spot analysis showed that the original model had a higher minimum and maximum shuttle rebound velocity comparing to the racket with alternated shaft stiffness. Moreover, a lower average velocity. This indicates that there is no linear connection for an optimal shaft stiffness regarding sweet spot and that a value close to that of the original model will give a higher maximum rebound shuttle velocity.

The results indicate that there is a possible gain in having a weaker shaft where greater racket head speeds at impacts are possible to achieve. However, this advantage probably does not outweigh the disadvantage of timing dependence and trajectory variation. This would explain that racket used by professionals usually have a higher shaft stiffness to cope with the increased speed of the game they play at.

5.4.4 Head Stiffness

As mentioned in Section 2.1.2 the influence from the head stiffness has not been studied extensively. Thus, it is hard to confirm the obtained results with results from other studies, although some physical phenomena are still identified. For instance, the re-bounce effect from the strings, measured as the COR value, is better for a stiffer head during the swing. The lower head stiffness deforms differently and is more sensitive to shear deflections at the impact time. The head stiffness also influences the string tension differently which is not evaluated within this report. In theory the head needs to be stiffer to withstand the force initialised from an increased string tension. Furthermore, the contact time increases with a weaker head which correlates to the fact that the strings need more time to stretch back as the head does not give the same support as a stiffer one.

From the simulation of the sweet spot it becomes clear that the stiffer head gives a higher tension in the head as it does not deform as much due to the stress initialisation in the strings. This results in a smaller sweet spot with similar maximum velocity but with a bigger gradient for the sweet spot drop off. Consequently, strokes far from the sweet spot centre have a lower velocity, i.e. the dead spot becomes larger. This could be beneficial for advanced players who prefer the ability to use drop balls close to the badminton net.

The values for the deflections when evaluating for the head stiffness gives different trends depending on the used stroke. The maximum deflection gives a clearer picture that the deflections are insignificant with a small indication that a weaker head gives a slightly more forward deflection, which is reasonable as a weaker material should result in an increased deformation. This is further confirmed by the racket velocity which is unaffected by the difference in head stiffness in the evaluated interval. The only deformable velocity significantly affected by the stiffness in the racket head is the rotational velocity which can be coupled with the difference in trajectory. The weak head gives less consistency over the string area when the racket is swung, resulting in shuttles that have a direction which is not perpendicular with the centred shuttle impact. The consistency is also better for the stiff head regarding different initial shuttle impacts for both evaluated strokes as the head will have a smaller deflection behaviour and thus the responses are less affected by how well the timing is in the stroke.

The result from this responses is an increased shuttle speed for a stiffer head as the COR value increases which correlates well with the re-bounce effect due to a more rigid head. As this is valid for both swings, however the trend needs further evaluation to capture stagnation points or other indicators showing an upper limit for the head stiffness.

5.4.5 Geometry

The geometry is interesting to evaluate not just from a performance perspective but also for a marketing aspect. Since the most common type on the market is the isometric shape it would be beneficial to find a head shape that is unique giving Salming the opportunity to create their own shape that will boost their name on the market.

For the two evaluated shapes there is a slightly increased forward deflection for the slower clear stroke, compared to the original racket, which gives an increased racket head velocity. The faster smash stroke does not

indicate the same behaviour. Hence, this effect is more significant for a slower stroke. Although, the angular deflection is less for both types of geometry comparing to the original racket, which indicates that the structure is more resistance to shearing deformations.

The Prince racket have better consistency for the slower stroke with a more straight trajectory and lowered standard deviation. However, at higher speed the opposite behaviour is captured which could be an effect from not hitting the smash at the optimum time. The Oval racket is more consistent for both strokes giving it a small advantage for the faster smash stroke. The result does indicate that both racket geometries have a slightly better consistence which could depend on the increased shear stiffness.

Regarding the shuttle speed there is a small advantage for the Prince racket when simulating the clear stroke which is not visible for the Oval racket. The COR value indicates similar behaviour giving the Prince racket a better effect from the string area. One reason why the differences is insignificant for the smash stroke, using the first initial simulation data, is explained by the velocity profile. In this profile it is illustrated that the smash stroke tends to be too early compared to where the maximum head velocity is in time.

By including the data for the later impact time the Prince racket have a higher velocity for the impact 2ms later. However the consistency in time reveals that timing is critical as the best performance is found within a interval of 2 ms, otherwise it gets out preformed by the original racket regarding shuttle speed. The results do not indicate why this results are so sensible to the impact time and needs further evaluation. For the Oval racket the second simulation further prove that the oval racket produces higher shuttle velocities for the smash which could be coupled to the better racket consistency as the trajectory is smoother for the oval racket.

By evaluating the sweet spot data from the Prince racket have the maximum re-bounce shuttle speed of over 15 m/s, to compare with the initial 20 m/s at impact. The re-bounce speed for the Oval racket is also higher than for the original racket although the drop of from the centre is more rapid than for the original. Why the Prince racket have the greatest performance in this simulation is due to the increased area of strings giving it a lager sweet spot but also reducing the drop of meaning that the shuttle velocity does not decrease as much as for the original racket when hitting the shuttle further away for the sweet spot centre.

5.5 FE-model and Material Properties

A distinct red line though all the results is the influence from the racket stiffness. Within this report the stiffness is governed by the material elastic stiffness. No evaluation of different layup sequences and orientations is included. As material properties is in many cases difficult to variate, due to limitation in available materials, the layup is an easier aspect to control. Furthermore, the angular deflection is an unwanted behaviour and it both from the shear stiffness in the head but also from the shaft. Thus, it is beneficial to include and increase the amount of ± 45 degree plies within the shaft stiffness. However, a careful evaluation of the stiffness is required as the shaft stiffness for bending highly affects the shuttle velocity and consistency of the stroke, thus 0 degrees plies must be included in the design.

The FE-model is well suited for the defined purpose although the computational cost is high. Thus, if further evaluations is done using more reduced elements and coarser mesh a larger amount of parameters can be evaluated. To be able to retain a model close to reality, the use of more detailed validations is required. Even though recommended values for mesh quality and time step was used, this can still influence the result due to the small variations of absolute values of the parametric values. Thus, an evaluation of the influence is interesting. Furthermore, the simulations used the double precision to increase the accuracy due to the large amounts of time steps yet the mesh convergence shows that a finer mesh is required. Thus, the error relation between mesh/result and double precision/result can influence the conclusions differently and it requires more investigation to properly weigh these settings against the computational cost.

5.6 Assumptions and Other Sources of Error

As mentioned above the results indicate several parameters that govern the behaviour of a racket. One must be aware that due to the different simplifications and assumptions made in the models and simulations, errors are present. Even though the evaluated results are analysed with these errors accounted for, the approach could be deficient to deal with this or something could have been missed that compromises the given result. Thus, it is important to know and understand the assumptions and simplifications when evaluating the result from the project.

The boundary condition used to simulate the motion introduce a clamped support for any other movements than the prescribed motions. Thus, vibrations otherwise absorbed by the hand are included in the results. To reduce this behaviour an approach could be to define a simplified model of the hand that have the motion applied to it and then to define a connection to the handle using springs and possible damping. This will prevent the clamped behaviour and instead have a more real case scenario. Although, since the vibrations are less significant during the acceleration phases, the result is still valid since the conclusions are done by evaluating the relative difference between the simulated models.

Regarding the applied motion given by the motion capture it was recorded for another type of racket. Hence, it is not certain that the exact swing would be possible with the simulated racket. Especially when changing the mass or COG, most likely the swing would differ regarding different rackets. Although, this simplification is needed for FE-analyses because otherwise each simulation would need its own motion capture data which is not effective in big data analyses or optimisation procedures.

Another assumption made was the choice of material as no material data was given. Hence, the model data was taken with reasonable properties for a badminton racket. A stiffness calibration pointing on a slightly lower stiffness and motion data for the top node was the two only calibration methods used. Thus, the material used could be far from what the given prototypes are constructed of. This is consider as a small issue as the relative data is still valid giving a demonstration of how tuning a specific material property would affect the different racket responses.

Furthermore, within this project the aerodynamic effects are neglected, i.e. the strokes are simulated in vacuum. In a true scenario the air resistance affect the deformation behaviour increasing the deflection during the acceleration phase. Hence, the velocities etc. would be affected as well. This would mostly affect different geometries as the other rackets have the same area facing the air but different angles depending on how the deflection behaves could introduce small differences. Thus, it would be beneficial to include the aerodynamic effects in another project. Additionally, the shuttle is simplified to a ball which in this case is a fairly good assumption. However, if the aerodynamic effects would be present the shuttle could benefit from a geometry closer to the real one since the ball shape introduces a spin which the feathers would brake. Hence, a more correct behaviour would be achieved using aerodynamic effects with a more correct geometry combined, but solely using a more accurate geometry would not affect the result significantly.

6

Conclusion

The purpose with this project was to identify key racket parameters that governs the racket dynamics during different strokes. This with the intention to prove that FEA is a valid method to improve the design process for a badminton racket. The smash and clear stroke were simulated, as these have high racket speeds whereby the change in a parameter should give a more noticeable effect on the result than other badminton strokes.

The method used was proven to be suitable for this type of simulation with recorded motions, using motion capture and building a FE-model used to simulate a corresponding stroke with LS-DYNA as an explicit FE-solver. Due to the lack of material data, a small bending test was made to calibrate the stiffness of the racket, which even after several evaluations still was too weak. However, to better understand how a change in a parameter alters the performance of a specific racket, the material data and composite layup needs to be known and validated against experimental tests. However, the results for the method defined in this thesis are valid for comparing different parameters, giving their relative influence of the racket dynamics. The used boundary condition, where the bottom of the handle on the racket was fixed to the motion controlled node, resulted in greater vibrations in the racket than is realistic. To reduce these a less rigid method to apply motions is needed, which would then better mimic the dampening effect of the hand. The influence of these vibrations did however decrease with greater acceleration and subsequently were negligible at impact. The FE-analysis does however simulate the swing motion and racket behaviour well, and with the suggested improvements FEA should be considered a valuable tool in badminton racket design. From the parametric study the influence of the design parameters are that:

- **Center of gravity** has a significant impact on the racket performance. With a higher COG the speed contribution from the deflection of the racket increases, resulting in higher shuttle velocities. This does however come at the expense of lessening consistency in performance, for instance a larger offset in the trajectory. It also requires more force to swing the racket. This could possibly be counteracted by a experienced and strong player. The lowering of the COG from the original model to the low COG model did not seem to impact the racket significantly, but did however show some benefit in shuttle trajectory variation.
- **Shaft stiffness** determines the rackets ability to resist bending during the swing. If timed well the re-deflection of the bent racket can contribute to the total racket velocity, producing higher shuttle velocities. The weaker shaft has the greatest shuttle velocity in the smash simulation when the impact time was shifted to suit the model better. This however points out the problem with the weak shaft model; it is very dependant on impact timing. The stiff shaft racket out-performed both the weak and the original model in consistency while performing similarly to the original racket in shuttle velocity. This explains why it is common for experienced players to use a stiffer shaft racket.
- **Head stiffness** affects the consistency of the stroke for the racket meaning that the racket becomes more or less dependent on the precision and timing during the stroke. A higher stiffness leads to a smaller sweet spot giving a lower average shuttle velocity if the impacts over the stringed area would be greatly distributed. For some, this is considered negative but it also increases the possibility to use the dead spot for short shuttle strokes. Additionally, a stiffer head means that the timing in the stroke is a bit less important and also the trajectory has less divergence from a clean hit giving the racket a more predictable response.
- **Mass** is the parameter affected the most by the used boundary condition for the motion as studies shows that a lighter and heavier rackets are swung differently due to their mass. Although, it is without doubt

that the lighter rackets are beneficial compared to the old wooden rackets but within intervals between lighter rackets the influence is not that obvious. The results indicate that regarding racket performance a lighter racket is better although this needs to be carefully validated with experimental data, thus the method needs improvement to validate this parameter.

- **Geometry** is maybe the most interesting parameter from a marketing point of view as it can give the racket its own unique design. Both the Oval racket and the Prince racket gives better shear stiffness which gives them a small advantage for slower strokes regarding consistency in trajectory. Otherwise, the Oval racket and the Original (Isometric) racket have similar racket performance which might explain why these two are the ones dominating the market. Regarding the Prince racket the peak values are better with higher max velocities and bigger Sweet spot. However, it is crucial that the timing in the stroke is correct as wrong timing could lead to lower velocities than for the other two racket. Consequently, it is a difficult racket to master but could be interesting to include in a design process to evaluate a unique design for a new production line. Maybe the consistency is better with a combination of higher head stiffness leading to an optimised racket with its own unique visual design.

7

Future Work

As badminton is a relative untouched subject for science, there are several approaches to identify interesting key properties of a badminton racket. But due to limitations some results fall outside the scope of this project, consequently complementary studies should to be done to fully capture how the parameters are influencing the characteristics of a badminton racket and more over how to optimise the racket for different players. The areas that need to be evaluated further can be divided into several points:

- The first aspect is regarding player styles and may be the most subjective part, thus it is hard to define objective values. A theory is that even if a racket is proven to be a bit faster in FE-simulations it might be unsuitable for a certain player style, further a player is able to adapt their strokes to the behaviour of the racket. Hence an experimental part needs to be included where physical models corresponding the simulated models are evaluated for different players and strokes using the motion capture.
- The second area that needs to be evaluated in order to enable optimisation is the behaviour when one or several parameters are combined. Does one affect another to be more or less significant regarding response and how can they be ranked against each other?
- To fully validate the simulations and used models whereby ensuring that the results are valid, calibrations against experimental data for the simulated parameters is required. Further the material data used in the physical model must correspond well with the simulated material when performing the calibration to have reliable results, something that was not possible within this project. It would also be of interest to evaluate the used composite to try different materials with other damping and stiffening properties. Maybe there exists a layup that could be consider to be optimal for a badminton racket and maybe the layup should be more divided into different sections of the racket with optimised layup respectively.
- The trends that are captured within this report should further be analysed to find the stagnated maximum for each parameter so that optimisation and weighting of these parameters are possible. Likewise the geometry could be further analysed using a wider spectra of different shapes and dimensions.
- Lastly the aerodynamic effects on both the shuttle and racket would be interesting to include, one theory is that the deflection would be largely affected by including the air resistance during the stroke. It would also be interesting to see if the behaviour remains if the shuttle would have its original shape.

References

- [1] C. Cohen and C. Clanet. Physics of ball sports. *Europhysics News* **47.3** (May 2016), 13–16. ISSN: 0531-7479, 1432-1092. DOI: 10.1051/epn/2016301. URL: <http://www.europhysicsnews.org/10.1051/epn/2016301> (visited on 01/17/2017).
- [2] Y. Liu. Project Application in the Field of Composite Materials in Badminton. *Applied Mechanics and Materials* **644-650** (2014), 4802–4804. ISSN: 1662-7482. DOI: 10.4028/www.scientific.net/AMM.644-650.4802. URL: <http://www.scientific.net.proxy.lib.chalmers.se/AMM.644-650.4802> (visited on 01/26/2017).
- [3] F. A. Nasruddin et al. *Finite element analysis on badminton racket design parameters*. OCLC: 920465951. 2016. ISBN: 978-3-319-21735-2. URL: <http://link.springer.com/content/pdf/10.1007%5C%2F978-3-319-21735-2.pdf> (visited on 01/17/2017).
- [4] M. Kwan. “Designing the world’s best badminton racket”. OCLC: 768330352. PhD thesis. Aalborg: Department of Mechanical and Manufacturing Engineering, Aalborg University, 2010.
- [5] N. Jamil. *Laws of badminton*. July 12, 2016. URL: http://system.bwf.website/documents/folder_1_81/Regulations/Laws/Part%20II%20Section%201A%20-%20Laws%20of%20Badminton%20-%20June%202016%20Revised%202.pdf (visited on 01/25/2017).
- [6] International Olympic Committee. *Badminton - Summer Olympic Sport*. International Olympic Committee. Jan. 11, 2017. URL: <https://www.olympic.org/badminton> (visited on 01/26/2017).
- [7] Encyclopaedia Britannica. *Battledore and shuttlecock*. *Encyclopaedia Britannica*. 11th ed. Vol. 1910-1911. 29 vols. Encyclopaedia Britannica 3. Cambridge University Press, 1910. URL: <http://www.gutenberg.org/files/34405/34405-h/34405-h.htm>.
- [8] Q. Zhu. Perceiving the affordance of string tension for power strokes in badminton: Expertise allows effective use of all string tensions. *Journal of Sports Sciences* **31.11** (July 2013), 1187–1196. ISSN: 0264-0414, 1466-447X. DOI: 10.1080/02640414.2013.771818. URL: <http://www.tandfonline.com/doi/abs/10.1080/02640414.2013.771818> (visited on 01/17/2017).
- [9] F. Alam et al. “A Comparative Study of Feather and Synthetic Badminton Shuttlecock Aerodynamics”. 17th Australasian Fluid Mechanics Conference. Australasian Fluid Mechanics Society, 2010, pp. 1–4. ISBN: 978-0-86869-129-9. URL: <https://researchbank.rmit.edu.au/view/rmit:13022> (visited on 01/27/2017).
- [10] Badminton World Federation. *Speed Tracker Ready for Smashing Success — BWF Fansite*. Mar. 26, 2015. URL: <http://bwfbadminton.com/2015/03/26/speed-tracker-ready-for-smashing-success/> (visited on 01/27/2017).
- [11] K. T. Lee, W. Xie, and K. C. Teh. “Notational analysis of international badminton competitions”. *ISBS - Conference Proceedings Archive*. 23 International Symposium on Biomechanics in Sports. Vol. 1. Beijing, Aug. 22, 2005. URL: <https://ojs.ub.uni-konstanz.de/cpa/article/view/799> (visited on 01/26/2017).

- [12] Y.-M. Tong and Y. Hong. “The playing pattern of world’s top single badminton players”. *ISBS - Conference Proceedings Archive*. 18 International Symposium on Biomechanics in Sports. Vol. 1. Hong Kong, June 25, 2000. URL: <https://ojs.ub.uni-konstanz.de/cpa/article/view/2234> (visited on 01/26/2017).
- [13] C.-C. Hsieh et al. “The effect of two different weighted badminton rackets about velocity and torque when outstanding badminton platers was preforming smash movement”. *ISBS - Conference Proceedings Archive*. 22 International Symposium on Biomechanics in Sports. Vol. 1. Ottawa, Aug. 8, 2004. URL: <https://ojs.ub.uni-konstanz.de/cpa/article/view/1350> (visited on 01/27/2017).
- [14] S. R. Michell, R. Jones, and M. A. King. Head speed vs. racket inertia in the tennis serve. *Sports Engineering* **3.2** (2001), 100–107. ISSN: <http://dx.doi.org/10.1046/j.1460-2687.2000.00051.x>. URL: https://www.researchgate.net/publication/229881539_Head_speed_vs_racket_inertia_in_the_tennis_serve (visited on 01/27/2017).
- [15] R. Cross and R. Bower. Effects of swing-weight on swing speed and racket power. *Journal of Sports Sciences* **24.1** (Jan. 2006), 23–30. ISSN: 0264-0414, 1466-447X. DOI: 10.1080/02640410500127876. URL: <http://www.tandfonline.com/doi/abs/10.1080/02640410500127876> (visited on 01/17/2017).
- [16] H. Brody. Player sensitivity to the moments of inertia of a tennis racket. *Sports Engineering* **3.2** (May 1, 2000), 145–148. ISSN: 1460-2687. DOI: 10.1046/j.1460-2687.2000.00054.x. URL: <http://onlinelibrary.wiley.com/doi/10.1046/j.1460-2687.2000.00054.x/abstract> (visited on 01/30/2017).
- [17] M. Kwan and J. Rasmussen. The importance of being elastic: Deflection of a badminton racket during a stroke. *Journal of Sports Sciences* **28.5** (Mar. 2010), 505–511. ISSN: 0264-0414, 1466-447X. DOI: 10.1080/02640410903567785. URL: <http://www.tandfonline.com/doi/abs/10.1080/02640410903567785> (visited on 01/17/2017).
- [18] R. Bower and R. Cross. String tension effects on tennis ball rebound speed and accuracy during playing conditions. *Journal of Sports Sciences* **23.7** (July 1, 2005), 765–771. ISSN: 0264-0414. DOI: 10.1080/02640410400021914. URL: <http://www-tandfonline-com.proxy.lib.chalmers.se/doi/abs/10.1080/02640410400021914> (visited on 01/30/2017).
- [19] R. Bower and R. Cross. Elite tennis player sensitivity to changes in string tension and the effect on resulting ball dynamics. *Sports Eng* **11.1** (Sept. 1, 2008), 31–36. ISSN: 1369-7072, 1460-2687. DOI: 10.1007/s12283-008-0006-z. URL: <http://link.springer.com/article/10.1007/s12283-008-0006-z> (visited on 01/30/2017).
- [20] R. Cross. The sweet spots of a tennis racquet. *Sports Engineering* **1.2** (Feb. 1, 1998), 63–78. ISSN: 1460-2687. DOI: 10.1046/j.1460-2687.1999.00011.x. URL: <http://onlinelibrary.wiley.com/doi/10.1046/j.1460-2687.1999.00011.x/abstract> (visited on 01/31/2017).
- [21] BETA CAE Systems. *ANSA version 16.2.x User’s Guide*. June 1, 2016.
- [22] Livermore Software Technology Corporation. “Hourglass (HG) Modes”. Apr. 11, 2012. URL: <http://ftp.lstc.com/anonymous/outgoing/jday/hourglass.pdf> (visited on 04/26/2017).
- [23] Andre Haufe, Karl Schweizerhof, and Paul DuBois. “Properties & Limits: Review of Shell Element Formulations”. Developer Forum 2013. Filderstadt/Germany, Sept. 24, 2013. URL: www.dynalook.com/Personally/af02_v10_elsaesser_trw_old.pdf.
- [24] Dr. -Ing. Ulrich Stelzmann. “Die grosse Elementbibliothek in LS-DYNA - Wann nimmt man was?” ANSYS Conferance & 28th CADFEM User’s Meeting 2010. Eurogress Aachen/Germany, Nov. 3, 2010. URL: http://www1.beuth-hochschule.de/~kleinsch/Expl_FEM/2010_Elementbibliothek_LSDyna_Cadfem.pdf.

- [25] B. D. Agarwal, L. J. Broutman, and K. Chandrashekhara. *Analysis and Performance of Fiber Composites*. 3 edition. Hoboken, N.J: Wiley, July 11, 2006. 576 pp. ISBN: 978-0-471-26891-8.
- [26] M. Fagerström. *Lecture notes: Composite Mechanics*. Feb. 29, 2016. URL: <https://pingpong.chalmers.se/courseId/6214/node.do?id=2898473&ts=1456767212558&u=914923836> (visited on 01/31/2017).
- [27] Livermore Software Technology Corporation. “Modeling of Composites in LS-DYNA”. Apr. 11, 2012. URL: http://ftp.lstc.com/anonymous/outgoing/jday/composites/mat_comp.pdf (visited on 05/08/2017).
- [28] Hawk-Eye. *Hawk-Eye Innovations Official Website*. Hawk-Eye Innovations Official Website. May 13, 2015. URL: <http://www.hawkeyeinnovations.co.uk/sports/badminton> (visited on 03/22/2017).
- [29] M. Kwan et al. Investigation of high-speed badminton racket kinematics by motion capture. *Sports Engineering* **13.2** (Jan. 2011), 57–63. ISSN: 1369-7072, 1460-2687. DOI: 10.1007/s12283-010-0053-0. URL: <http://link.springer.com/10.1007/s12283-010-0053-0> (visited on 01/17/2017).
- [30] M. Kwan et al. Measurement of badminton racket deflection during a stroke. *Sports Engineering* **12.3** (May 2010), 143–153. ISSN: 1369-7072, 1460-2687. DOI: 10.1007/s12283-010-0040-5. URL: <http://link.springer.com/10.1007/s12283-010-0040-5> (visited on 01/17/2017).
- [31] S. P. Silva et al. Cork: properties, capabilities and applications. *International Materials Reviews* **50.6** (Nov. 29, 2013), 345–365. ISSN: 0950-6608. DOI: 10.1179/174328005X41168. URL: <http://dx.doi.org/10.1179/174328005X41168> (visited on 01/30/2017).
- [32] Livermore Software Technology Corporation and DYNAmore. *Consistent units*. Nov. 25, 2016. URL: <http://www.dynasupport.com/howtos/general/consistent-units> (visited on 05/08/2017).
- [33] Livermore Software Technology Corporation. *LS-DYNA Keyword User’s Manual, Volume II, Material Models, Version 971*. Mar. 26, 2012. URL: www.lstc.com.
- [34] M. Andersson and E. Larsson. *Benchmarking study of steel-composite structures in CAE crash applications*. Chalmers studentarbeten. 2016. URL: <http://studentarbeten.chalmers.se> (visited on 03/29/2017).
- [35] L. Li et al. Effects of string tension and impact location on tennis playing. *J Mech Sci Technol* **23.11** (Nov. 1, 2009), 2990–2997. ISSN: 1738-494X, 1976-3824. DOI: 10.1007/s12206-009-0903-5. URL: <http://link.springer.com/article/10.1007/s12206-009-0903-5> (visited on 01/31/2017).

A

Tables

The complete results for all shuttles presented for the clear swing.

	Avg	Stddev	Shuttle1	Shuttle2	Shuttle3	Shuttle4	Shuttle5	Shuttle6	Shuttle7
Original	45.1 m/s	3.64 m/s	46.4 m/s	49.1 m/s	48.3 m/s	43.1 m/s	42.7 m/s	46.9 m/s	38.9 m/s
Stiff shaft	45.4 m/s	3.75 m/s	46.8 m/s	49.9 m/s	48 m/s	43.3 m/s	43.4 m/s	47.8 m/s	39 m/s
Weak shaft	44.1 m/s	3.89 m/s	45.7 m/s	48.3 m/s	47.7 m/s	42.5 m/s	40 m/s	46.2 m/s	38.3 m/s
Stiff head	45.4 m/s	3.87 m/s	46.7 m/s	49.7 m/s	48.6 m/s	43.2 m/s	42.8 m/s	47.7 m/s	38.9 m/s
Weak head	43.6 m/s	3.49 m/s	45.2 m/s	47.6 m/s	46.6 m/s	42.2 m/s	40.6 m/s	45.4 m/s	37.9 m/s
High COG	49.2 m/s	3.96 m/s	50.2 m/s	54 m/s	49.5 m/s	46.8 m/s	48.7 m/s	53 m/s	42.1 m/s
Low COG	45.9 m/s	3.8 m/s	47.5 m/s	50.4 m/s	48.2 m/s	43.8 m/s	43.8 m/s	48 m/s	39.2 m/s
High mass	41.9 m/s	3.55 m/s	43.3 m/s	45.7 m/s	45.2 m/s	40 m/s	38.6 m/s	44 m/s	36.4 m/s
Low mass	45.5 m/s	3.76 m/s	46.9 m/s	50.1 m/s	47.9 m/s	43.5 m/s	43.3 m/s	47.6 m/s	38.9 m/s
Prince	47.8 m/s	3.89 m/s	49.2 m/s	52.4 m/s	50.2 m/s	45.7 m/s	45.1 m/s	50.8 m/s	41.4 m/s
Oval	45.1 m/s	3.64 m/s	46.4 m/s	49.1 m/s	48.3 m/s	43.1 m/s	42.7 m/s	46.9 m/s	38.9 m/s

Table A.1: The difference in speed of the ball post impact compared to the original racket in the clearwing. In meters per second.

	Avg	Stddev	Shuttle1	Shuttle2	Shuttle3	Shuttle4	Shuttle5	Shuttle6	Shuttle7
Original	0.62	0.14	0.69	0.75	0.76	0.54	0.57	0.66	0.38
Stiff shaft	0.65	0.14	0.74	0.79	0.77	0.57	0.60	0.70	0.40
Weak shaft	0.51	0.12	0.63	0.59	0.64	0.50	0.36	0.52	0.36
Stiff head	0.63	0.14	0.70	0.77	0.77	0.55	0.57	0.68	0.38
Weak head	0.57	0.13	0.66	0.69	0.69	0.52	0.50	0.61	0.35
High COG	0.70	0.15	0.73	0.89	0.70	0.63	0.62	0.89	0.46
Low COG	0.67	0.14	0.75	0.83	0.75	0.59	0.62	0.75	0.41
High mass	0.52	0.15	0.57	0.66	0.67	0.45	0.35	0.63	0.31
Low mass	0.67	0.14	0.73	0.83	0.75	0.59	0.61	0.74	0.40
Prince	0.71	0.14	0.76	0.86	0.79	0.63	0.64	0.82	0.46
Oval	0.62	0.14	0.69	0.75	0.76	0.54	0.57	0.66	0.38

Table A.2: Coefficient of restitution.

	Avg	Stddev	Shuttle1	Shuttle2	Shuttle3	Shuttle4	Shuttle5	Shuttle6	Shuttle7
Original	0.873 deg	0.636 deg	0 deg	0.506 deg	1.94 deg	0.0386 deg	0.775 deg	0.916 deg	1.06 deg
Stiff shaft	0.7 deg	0.599 deg	0 deg	0.732 deg	1.86 deg	0.463 deg	0.141 deg	0.438 deg	0.568 deg
Weak shaft	0.861 deg	0.528 deg	0 deg	1.12 deg	0.0545 deg	0.388 deg	0.974 deg	1.43 deg	1.2 deg
Stiff head	0.772 deg	0.716 deg	0 deg	0.541 deg	2.19 deg	0.293 deg	0.319 deg	0.55 deg	0.733 deg
Weak head	0.9 deg	0.578 deg	0 deg	1.05 deg	0.59 deg	0.488 deg	0.171 deg	1.61 deg	1.49 deg
High COG	0.826 deg	0.409 deg	0 deg	1.01 deg	1.49 deg	0.347 deg	0.464 deg	0.858 deg	0.788 deg
Low COG	0.698 deg	0.364 deg	0 deg	0.861 deg	1.12 deg	0.266 deg	0.485 deg	0.393 deg	1.06 deg
High mass	0.647 deg	0.418 deg	0 deg	0.568 deg	0.825 deg	0.148 deg	0.197 deg	1.17 deg	0.976 deg
Low mass	0.6 deg	0.283 deg	0 deg	0.726 deg	0.534 deg	0.484 deg	0.19 deg	0.617 deg	1.05 deg
Prince	0.275 deg	0.155 deg	0 deg	0.27 deg	0.288 deg	0.467 deg	0.384 deg	0.228 deg	0.0136 deg
Oval	0.873 deg	0.636 deg	0 deg	0.506 deg	1.94 deg	0.0386 deg	0.775 deg	0.916 deg	1.06 deg

Table A.3: The offset in shuttle trajectory post impact, measured from ball 1 trajectory in the horizontal plane, in the clear swing.

	Avg	Stddev	Ball1	Ball2	Ball3	Ball4	Ball5	Ball6	Ball7
Original	480.81 ms	0.29 ms	480.8 ms	480.78 ms	481.32 ms	480.84 ms	480.32 ms	480.72 ms	480.86 ms
Stiff shaft	+0.06 ms	-0.03 ms	+0.06 ms	+0.06 ms	+0 ms	+0.06 ms	+0.1 ms	+0.09 ms	+0.05 ms
Weak shaft	-0.79 ms	+0.05 ms	-0.8 ms	-0.86 ms	-0.72 ms	-0.73 ms	-0.84 ms	-0.9 ms	-0.67 ms
Stiff head	+0 ms	-0.01 ms	+0 ms	+0.02 ms	-0.02 ms	+0.01 ms	+0.01 ms	+0.03 ms	-0.01 ms
Weak head	+0 ms	+0.06 ms	+0 ms	+0 ms	+0.08 ms	+0.01 ms	-0.12 ms	+0.01 ms	-0.01 ms
High COG	-0.49 ms	-0.03 ms	-0.49 ms	-0.54 ms	-0.56 ms	-0.46 ms	-0.39 ms	-0.56 ms	-0.41 ms
Low COG	-0.04 ms	-0.1 ms	-0.04 ms	-0.06 ms	-0.23 ms	-0.03 ms	+0.14 ms	-0.06 ms	-0.02 ms
High mass	-0.27 ms	+0.11 ms	-0.27 ms	-0.31 ms	-0.1 ms	-0.24 ms	-0.46 ms	-0.33 ms	-0.21 ms
Low mass	-0.04 ms	-0.09 ms	-0.04 ms	-0.05 ms	-0.21 ms	-0.02 ms	+0.13 ms	-0.06 ms	-0.02 ms
Prince	-0.12 ms	-0.1 ms	-0.12 ms	-0.14 ms	-0.31 ms	-0.09 ms	+0.08 ms	-0.16 ms	-0.08 ms
Oval	+0 ms	+0 ms	+0 ms	+0 ms	+0 ms	+0 ms	+0 ms	+0 ms	+0 ms

Table A.4: The time difference when the shuttle first makes contact with the racket in the clear swing.

	Avg	Stddev	Shuttle1	Shuttle2	Shuttle3	Shuttle4	Shuttle5	Shuttle6	Shuttle7
Original	1.32 ms	0.069 ms	1.35 ms	1.33 ms	1.3 ms	1.39 ms	1.37 ms	1.18 ms	1.32 ms
Stiff shaft	1.31 ms	0.074 ms	1.34 ms	1.32 ms	1.29 ms	1.36 ms	1.37 ms	1.15 ms	1.31 ms
Weak shaft	1.31 ms	0.078 ms	1.38 ms	1.32 ms	1.34 ms	1.38 ms	1.29 ms	1.15 ms	1.31 ms
Stiff head	1.31 ms	0.074 ms	1.36 ms	1.32 ms	1.29 ms	1.37 ms	1.37 ms	1.16 ms	1.32 ms
Weak head	1.34 ms	0.073 ms	1.37 ms	1.35 ms	1.34 ms	1.41 ms	1.4 ms	1.19 ms	1.35 ms
High COG	1.31 ms	0.068 ms	1.34 ms	1.32 ms	1.34 ms	1.38 ms	1.34 ms	1.17 ms	1.3 ms
Low COG	1.28 ms	0.078 ms	1.3 ms	1.28 ms	1.28 ms	1.35 ms	1.33 ms	1.11 ms	1.29 ms
High mass	1.35 ms	0.072 ms	1.4 ms	1.37 ms	1.37 ms	1.39 ms	1.38 ms	1.19 ms	1.34 ms
Low mass	1.27 ms	0.074 ms	1.31 ms	1.27 ms	1.26 ms	1.34 ms	1.33 ms	1.12 ms	1.29 ms
Prince	1.32 ms	0.089 ms	1.34 ms	1.3 ms	1.32 ms	1.4 ms	1.36 ms	1.13 ms	1.37 ms
Oval	1.32 ms	0.069 ms	1.35 ms	1.33 ms	1.3 ms	1.39 ms	1.37 ms	1.18 ms	1.32 ms

Table A.5: The difference in length of contact for the different impacts in the clear swing, compared to original racket.

The complete results for all shuttles presented for the smash swing.

	Avg	Stddev	Shuttle1	Shuttle2	Shuttle3	Shuttle4	Shuttle5	Shuttle6	Shuttle7
Original	57.3 m/s	4.02 m/s	59.8 m/s	62.6 m/s	58.6 m/s	56 m/s	55.9 m/s	58.7 m/s	49.8 m/s
Stiff shaft	58 m/s	4.05 m/s	60.6 m/s	63.1 m/s	59.7 m/s	56.4 m/s	56.6 m/s	59 m/s	50.4 m/s
Weak shaft	63.9 m/s	6.81 m/s	67.8 m/s	69.9 m/s	70.2 m/s	61.9 m/s	67.2 m/s	51.8 m/s	58.7 m/s
Stiff head	58.1 m/s	4.13 m/s	60.5 m/s	63.4 m/s	59.1 m/s	56.4 m/s	57 m/s	59.7 m/s	50.3 m/s
Weak head	55.7 m/s	3.75 m/s	58.2 m/s	60.6 m/s	57.2 m/s	54.6 m/s	54 m/s	56.4 m/s	48.8 m/s
High COG	61.2 m/s	6.18 m/s	64.9 m/s	69.8 m/s	66.3 m/s	60.7 m/s	58.8 m/s	53.9 m/s	53.6 m/s
Low COG	57.4 m/s	3.84 m/s	60.6 m/s	62.1 m/s	57.4 m/s	56.3 m/s	58 m/s	57.7 m/s	50 m/s
High mass	53.9 m/s	4.33 m/s	56.2 m/s	59.1 m/s	56.4 m/s	52.7 m/s	49.9 m/s	56.1 m/s	46.7 m/s
Low mass	56.6 m/s	3.77 m/s	59.5 m/s	61.4 m/s	56.8 m/s	55.4 m/s	56.9 m/s	56.5 m/s	49.3 m/s
Prince	57.2 m/s	4.62 m/s	59.4 m/s	62.9 m/s	60 m/s	55.7 m/s	53.1 m/s	59.8 m/s	49.7 m/s
Oval	57.3 m/s	4.17 m/s	59.9 m/s	62.8 m/s	58.4 m/s	55.6 m/s	55.8 m/s	59.1 m/s	49.7 m/s

Table A.6: The difference in speed of the ball post impact compared to the original racket in the smashwing. In meters per second.

	Avg	Stddev	Shuttle1	Shuttle2	Shuttle3	Shuttle4	Shuttle5	Shuttle6	Shuttle7
Original	0.40	0.12	0.43	0.56	0.46	0.32	0.38	0.46	0.18
Stiff shaft	0.48	0.13	0.58	0.63	0.53	0.46	0.42	0.53	0.24
Weak shaft	0.44	0.17	0.55	0.60	0.58	0.41	0.47	0.11	0.34
Stiff head	0.42	0.13	0.45	0.58	0.48	0.33	0.40	0.48	0.19
Weak head	0.36	0.11	0.40	0.51	0.42	0.29	0.33	0.40	0.16
High COG	0.35	0.14	0.44	0.53	0.49	0.33	0.33	0.18	0.18
Low COG	0.46	0.13	0.57	0.60	0.47	0.44	0.44	0.48	0.20
High mass	0.29	0.10	0.36	0.39	0.38	0.25	0.22	0.32	0.10
Low mass	0.44	0.13	0.55	0.58	0.46	0.43	0.42	0.45	0.19
Prince	0.40	0.11	0.48	0.51	0.51	0.35	0.32	0.42	0.20
Oval	0.41	0.13	0.45	0.58	0.47	0.33	0.38	0.47	0.19

Table A.7: Coefficient of restitution.

	Avg	Stddev	Shuttle1	Shuttle2	Shuttle3	Shuttle4	Shuttle5	Shuttle6	Shuttle7
Original	0.655 deg	0.825 deg	0 deg	0.0208 deg	1.06 deg	0.347 deg	0.0306 deg	2.15 deg	0.318 deg
Stiff shaft	0.57 deg	0.748 deg	0 deg	0.289 deg	0.0535 deg	0.291 deg	0.553 deg	2.06 deg	0.175 deg
Weak shaft	1.57 deg	1.51 deg	0 deg	0.165 deg	1.01 deg	0.746 deg	1.99 deg	4.41 deg	1.13 deg
Stiff head	0.451 deg	0.414 deg	0 deg	0.25 deg	1.03 deg	0.346 deg	0.0281 deg	0.901 deg	0.153 deg
Weak head	1.03 deg	0.767 deg	0 deg	0.0175 deg	0.751 deg	0.887 deg	0.712 deg	2.23 deg	1.57 deg
High COG	3.1 deg	6.29 deg	0 deg	0.23 deg	0.24 deg	0.411 deg	1.07 deg	15.9 deg	0.698 deg
Low COG	0.634 deg	0.576 deg	0 deg	0.387 deg	1.38 deg	0.124 deg	0.0866 deg	1.32 deg	0.508 deg
High mass	0.749 deg	0.811 deg	0 deg	0.024 deg	0.566 deg	0.32 deg	1.35 deg	2.1 deg	0.143 deg
Low mass	0.773 deg	0.628 deg	0 deg	0.567 deg	1.54 deg	0.205 deg	0.0377 deg	1.46 deg	0.826 deg
Prince	0.783 deg	0.78 deg	0 deg	0.256 deg	0.476 deg	0.104 deg	1.61 deg	1.93 deg	0.324 deg
Oval	0.484 deg	0.483 deg	0 deg	0.551 deg	0.0134 deg	0.0211 deg	0.627 deg	1.32 deg	0.373 deg

Table A.8: The offset in shuttle trajectory post impact, measured from ball 1 trajectory in the horizontal plane, in the smash swing.

	Avg	Stddev	Ball1	Ball2	Ball3	Ball4	Ball5	Ball6	Ball7
Original	591.94 ms	0.28 ms	591.93 ms	592.02 ms	592.36 ms	591.9 ms	591.47 ms	592.1 ms	591.77 ms
Stiff shaft	+0.14 ms	-0.01 ms	+0.14 ms	+0.18 ms	+0.11 ms	+0.13 ms	+0.17 ms	+0.18 ms	+0.11 ms
Weak shaft	+0.31 ms	-0.09 ms	+0.31 ms	+0.32 ms	+0.16 ms	+0.32 ms	+0.49 ms	+0.28 ms	+0.32 ms
Stiff head	+0.01 ms	-0.01 ms	+0.01 ms	+0.01 ms	-0.01 ms	+0.01 ms	+0.02 ms	+0 ms	+0.01 ms
Weak head	-0.02 ms	+0.03 ms	-0.02 ms	+0 ms	+0.02 ms	-0.01 ms	-0.07 ms	-0.01 ms	-0.02 ms
High COG	-0.1 ms	+0.02 ms	-0.09 ms	-0.11 ms	-0.05 ms	-0.07 ms	-0.15 ms	-0.14 ms	-0.05 ms
Low COG	+0.11 ms	-0.03 ms	+0.1 ms	+0.12 ms	+0.04 ms	+0.1 ms	+0.18 ms	+0.12 ms	+0.1 ms
High mass	-0.14 ms	+0.07 ms	-0.14 ms	-0.14 ms	-0.02 ms	-0.12 ms	-0.28 ms	-0.15 ms	-0.12 ms
Low mass	+0.13 ms	-0.02 ms	+0.12 ms	+0.14 ms	+0.08 ms	+0.12 ms	+0.17 ms	+0.14 ms	+0.11 ms
Prince	-0.23 ms	-0.01 ms	-0.23 ms	-0.26 ms	-0.23 ms	-0.21 ms	-0.23 ms	-0.25 ms	-0.19 ms
Oval	-0.02 ms	+0 ms	-0.02 ms	-0.01 ms	-0.03 ms	-0.02 ms	-0.02 ms	-0.02 ms	-0.03 ms

Table A.9: The time difference when the shuttle first makes contact with the racket in the smash swing.

	Avg	Stddev	Shuttle1	Shuttle2	Shuttle3	Shuttle4	Shuttle5	Shuttle6	Shuttle7
Original	1.2 ms	0.102 ms	1.25 ms	1.22 ms	1.14 ms	1.3 ms	1.27 ms	1 ms	1.23 ms
Stiff shaft	1.2 ms	0.116 ms	1.26 ms	1.2 ms	1.14 ms	1.3 ms	1.29 ms	0.97 ms	1.25 ms
Weak shaft	1.24 ms	0.062 ms	1.3 ms	1.26 ms	1.17 ms	1.34 ms	1.21 ms	1.2 ms	1.2 ms
Stiff head	1.2 ms	0.105 ms	1.24 ms	1.21 ms	1.13 ms	1.29 ms	1.28 ms	0.99 ms	1.23 ms
Weak head	1.23 ms	0.105 ms	1.28 ms	1.23 ms	1.15 ms	1.32 ms	1.32 ms	1.03 ms	1.27 ms
High COG	1.28 ms	0.073 ms	1.26 ms	1.23 ms	1.21 ms	1.3 ms	1.3 ms	1.43 ms	1.25 ms
Low COG	1.17 ms	0.108 ms	1.25 ms	1.17 ms	1.11 ms	1.25 ms	1.26 ms	0.96 ms	1.2 ms
High mass	1.26 ms	0.099 ms	1.28 ms	1.26 ms	1.2 ms	1.36 ms	1.35 ms	1.07 ms	1.29 ms
Low mass	1.16 ms	0.103 ms	1.23 ms	1.16 ms	1.09 ms	1.23 ms	1.25 ms	0.96 ms	1.19 ms
Prince	1.25 ms	0.101 ms	1.27 ms	1.28 ms	1.22 ms	1.33 ms	1.29 ms	1.03 ms	1.3 ms
Oval	1.19 ms	0.107 ms	1.24 ms	1.17 ms	1.12 ms	1.27 ms	1.27 ms	0.98 ms	1.25 ms

Table A.10: The difference in length of contact for the different impacts in the smash swing, compared to original racket.

B

Sweet Spots

The simulated sweet spot for the fixed racket with the first picture illustrated the different shuttle position used to interpolate the sweet spot. Initial shuttle velocity of 20 m/s.

